





Overexpression of *TaSTT3b-2B* improves resistance to sharp eyespot and increases grain weight in wheat

Xiuliang Zhu^{1,*} , Wei Rong¹, Kai Wang¹, Wei Guo², Miaoping Zhou², Jizhong Wu², Xingguo Ye¹ , Xuening Wei¹  and Zengyan Zhang^{1,*} 

¹Key Laboratory of Biology and Genetic Improvement of Triticeae Crops, Ministry of Agriculture/The National Key Facility for Crop Gene Resources and Genetic Improvement, Institute of Crop Sciences, Chinese Academy of Agricultural Sciences, Beijing, China

²Jiangsu Academy of Agricultural Sciences, Nanjing, China

Received 26 May 2021;
revised 5 November 2021;
accepted 28 November 2021.

*Correspondence (Tel +86 10 82108546;
fax +86 10 82105819; email
zhuxiuliang@caas.cn; Tel +86 10 82108781;
fax +86 10 82105819; email
zhangzengyan@caas.cn)

Keywords: Grain weight, jasmonic acid, *Rhizoctonia cerealis*, STAUROSPORINE AND TEMPERATURE SENSITIVE3 (STT3), transgenic wheat, *Triticum aestivum*.

Summary

STAUROSPORINE AND TEMPERATURE SENSITIVE3 (STT3) is a catalytic subunit of oligosaccharyltransferase, which is important for asparagine-linked glycosylation. Sharp eyespot, caused by the necrotrophic fungal pathogen *Rhizoctonia cerealis*, is a devastating disease of bread wheat. However, the molecular mechanisms underlying wheat defense against *R. cerealis* are still largely unclear. In this study, we identified *TaSTT3a* and *TaSTT3b*, two STT3 subunit genes from wheat and reported their functional roles in wheat defense against *R. cerealis* and increasing grain weight. The transcript abundance of *TaSTT3b-2B* was associated with the degree of wheat resistance to *R. cerealis* and induced by both *R. cerealis* and exogenous jasmonic acid (JA). Overexpression of *TaSTT3b-2B* significantly enhanced resistance to *R. cerealis*, grain weight, and JA content in transgenic wheat subjected to *R. cerealis* stress, while silencing of *TaSTT3b-2B* compromised resistance of wheat to *R. cerealis*. Transcriptomic analysis showed that *TaSTT3b-2B* affected the expression of a series of defense-related genes and JA biosynthesis-related genes, as well as genes coding starch synthase and sucrose synthase. Application of exogenous JA elevated expression levels of the abovementioned defense- and grain weight-related genes, and rescuing the resistance of *TaSTT3b-2B*-silenced wheat to *R. cerealis*, while pretreatment with sodium diethyldithiocarbamate, an inhibitor of JA synthesis, attenuated the *TaSTT3b-2B*-mediated resistance to *R. cerealis*, suggesting that *TaSTT3b-2B* played critical roles in regulating *R. cerealis* resistance and grain weight via JA biosynthesis. Altogether, this study reveals new functional roles of *TaSTT3b-2B* in regulating plant innate immunity and grain weight, and illustrates its potential application value for wheat molecular breeding.

Introduction

The wheat sharp eyespot disease, primarily caused by *Rhizoctonia cerealis*, is a destructive disease of wheat in warm humid regions of the world, including China (Chen *et al.*, 2008, 2013), the United Kingdom (Clarkson and Cook, 1983), New Zealand (Cromey *et al.*, 2002), and Egypt (Hammouda, 2003). Dark-bordered lesions appear on the stem bases of young and mature wheat plants about seven days after infection by *R. cerealis*. Subsequently, peduncle rot occurs, leading to lodging at the internode and even premature spike senescence or ripening, which is also known as white heads (Ren *et al.*, 2020). Although chemical control is available for wheat fungal pathogens, fungicide resistance has become increasingly prominent due to long-term use of a single chemical fungicide (Chen *et al.*, 2007). Breeding resistant cultivars with resistance against *R. cerealis* is a more cost-effective and environmental friendly alternative. Therefore, it is urgent to identify genes that play important roles in plant defense response and unravel their underlying functional mechanisms. Although few quantitative trait loci (QTLs) have been reported to be associated with resistance to sharp eyespot disease in wheat (Chen *et al.*, 2013; Wu *et al.*, 2017), no QTL has

been applied to molecular breeding. Thus, the molecular basis for the defense and signaling pathways that underlie the interaction between the host wheat with *R. cerealis* remains largely unknown.

Asparagine N-glycosylation is a major class of posttranslational modification, which is catalyzed by the oligosaccharyltransferase (OST) complex in the lumen of the endoplasmic reticulum (ER). In plants, N-glycosylation has been shown to play vital roles in diverse aspects of development and physiology, including salt tolerance and plant immunity (Häweker *et al.*, 2010; Jia *et al.*, 2020; Jiao *et al.*, 2020; Koiwa *et al.*, 2003; Lerouge *et al.*, 1998; Liebminger *et al.*, 2009; Liu and Howell, 2010; Nagashima *et al.*, 2018; Saijo *et al.*, 2009). As one subunit of the OST complex, the STAUROSPORINE AND TEMPERATURE SENSITIVE3 (STT3) subunit is critical for the catalytic activity of OST that transfers a preassembled glycan chain (Glc3Man9GlcNAc2) to a special asparagine residue in the sequon N-X-Ser/Thr (X is except Pro) of acceptor proteins (Aebi, 2013; Lu *et al.*, 2018; Ruiz-Canada *et al.*, 2009). Mammalian cells contain two isoforms of STT3. STT3a is primarily required for co-translational glycosylation of the nascent polypeptide and STT3a can also mediate posttranslational glycosylation of the sites that have been missed by STT3a (Ruiz-Canada

et al., 2009). In the model plant *Arabidopsis*, there also exists two STT3 isoforms (STT3a and STT3b). Koiwa et al. (2003) reported that each single mutant of *STT3a* and *STT3b* was viable, but the double mutant *stt3a stt3b* was gametophytic lethal. The *stt3a* mutant displays a defect of reduced glycosylation of proteins, affecting cell wall biosynthesis and leading to compromised abiotic stress tolerance; however, *stt3b* mutant plants do not show a similar phenotype of reduced glycosylation (Häweker et al., 2010; Koiwa et al., 2003). Interestingly, the *STT3a* gene cloned from *Spartina alterniflora* completely complements the salt-sensitive phenotype of the *Arabidopsis stt3a* mutant (Jiang et al., 2015), suggesting that both *STT3a* genes are conserved in the two plant species. All these studies imply that STT3a is essential for N-glycosylation and stress tolerance of plants (Jeong et al., 2018; Koiwa et al., 2003). In *Arabidopsis*, BRASSINOSTEROID INSENSITIVE 1-associated receptor kinase 1 (BAK1), somatic embryogenesis receptor kinase4 (SERK4), and BAK1-INTERACTING RECEPTOR-LIKE KINASE 1 (BIR1) negatively regulate the process of cell death (He et al., 2007; Kemmerling et al., 2007; Gao et al., 2009), and STT3a was identified as an important regulator of bak1/serk4 cell death (de Oliveira et al., 2016). In the *stt3a* mutant, the functions of the receptor kinase EF-TU RECEPTOR1 (Häweker et al., 2010) and the BAK1/SERK4 pathway (de Oliveira et al., 2016) involved in plant innate immunity pathways were impaired. Similarly, loss of function of *STT3a* also suppressed the autoimmune phenotype in *bir1-1* (Zhang et al., 2015). The latest research indicated that a mutation in *STT3a* impaired N-glycosylation and showed greater susceptibility to *Pst* DC3000 infection (Jia et al., 2020). However, little is known about the involvement of STT3 in defense responses of wheat against various pathogens.

Jasmonic acid (JA) signaling pathways have been reported to induce resistance against necrotrophs, such as *Alternaria brassicicola* (Chen et al., 2021; Thomma et al., 1998), *Botrytis cinerea* (Chen et al., 2021; Liu et al., 2019), *Bipolaris sorokiniana* (Singh et al., 2019), and *R. solani* (Taheri and Tarighi, 2010). In rice (*Oryza sativa*), *cpm2* and *hebiba* mutants, which are defective for allene oxide cyclase activity and JA production, show increased susceptibility to *Magnaporthe oryzae*. Application of exogenous JA restored resistance to *M. oryzae* in these mutants, suggesting that JA was required for this response (Riemann et al., 2013). Exogenous JA application to rice also induced resistance against *R. solani* (Taheri and Tarighi, 2010).

In recent years, a number of major QTLs and regulatory genes, which control grain size and grain weight of wheat, have been isolated. These cloned grain weight-related genes can be divided into several types, such as serine carboxypeptidase, ubiquitin E3 RING ligase, G protein, sucrose synthase, ubiquitin receptor, mitogen-activated protein kinase, purine permease, and B3-type transcription factor (Hou et al., 2014; Li et al., 2008, 2011, 2021; Su et al., 2011; Sun et al., 2018; Xia et al., 2013; Xu et al., 2018; Yin et al., 2020). Nevertheless, no study has reported the regulatory role of STT3 in grain weight. As an essential plant hormone, JA plays critical roles in plant defense and development (Lyons et al., 2013). However, studies about JA involved in regulation of grain weight are scarce.

In this study, we identified two STT3 subunit genes *TaSTT3a* and *TaSTT3b* in wheat and provided evidence that *TaSTT3b-2B* positively regulated defense against *R. cerealis*. We explored the mechanism underlying *TaSTT3b-2B*-mediated resistance to *R. cerealis*, in which *TaSTT3b-2B* enhanced the transcript levels of various defense-related genes. *TaSTT3b-2B* also affected the

JA content and the expression of JA synthesis-related genes, and application of exogenous JA increased resistance to *R. cerealis*, whereas pretreatment with sodium diethyldithiocarbamate (DIECA), an inhibitor of JA synthesis, reduced the *TaSTT3b-2B*-mediated resistance to *R. cerealis*. Furthermore, we found that *TaSTT3b-2B* overexpression up-regulated the expression of the starch synthase and sucrose synthase genes, leading to larger grains produced in transgenic wheat infected with *R. cerealis*. Thus, our results indicate an essential role of *TaSTT3b-2B* in wheat defense response to *R. cerealis* and in controlling grain size, and overall, its potential application in wheat molecular breeding.

Results

Identification and expression patterns of *TaSTT3a* and *TaSTT3b* genes in common wheat

STT3 plays important roles in abiotic stress tolerance of the host plants (Jiang et al., 2015; Jiao et al., 2020; Koiwa et al., 2003). Here, we explored whether STT3 in common wheat is involved in defense response to biotic stress. To obtain the sequences of *STT3* genes in wheat, we conducted BLAST searches against IWGSC Survey Sequence Assemblies using the amino acid sequences of STT3a (AAL07040.1) and STT3b (NP_174675.2) in *Arabidopsis* as seed sequences. Six highly conserved, full sequences (TraesCS1A02G340400.1, TraesCS1B02G352700.1, and TraesCS1D02G342400.1 conserved to STT3a; and TraesCS2A02G555600.1, TraesCS2B02G587900.1, and TraesCS2D02G558800.1 conserved to STT3b) were obtained, indicating that the wheat *STT3a* and *STT3b* genes each had three homologous loci (named as *TaSTT3a-1A*, *TaSTT3a-1B*, *TaSTT3a-1D*, *TaSTT3b-2A*, *TaSTT3b-2B*, and *TaSTT3b-2D* in this study) on the A, B, and D chromosomes. To investigate the role of STT3 in wheat defense against pathogen infection, we detected the expression profiles of *TaSTT3a* and *TaSTT3b* in wheat after *R. cerealis* infection using real-time quantitative PCR (qRT-PCR). The results showed that the transcriptional abundance of *TaSTT3b* was significantly elevated after *R. cerealis* infection, and the induced level of *TaSTT3b-2B* was the highest at 10 days post infection (dpi) with *R. cerealis* (Figure 1a). While transcriptional levels of *TaSTT3a* were only up-regulated at 10 dpi and 21 dpi, the induction degree was relatively weaker than that of *TaSTT3b-2B* (Figure S1).

Because *TaSTT3b-2B* had extremely high identities with *TaSTT3b-2A* (99.45%) and *TaSTT3b-2D* (99.59%) in their amino acid sequences (Figure S2, Table S1), and *TaSTT3b-2B* had the highest expression level in wheat after *R. cerealis* infection, *TaSTT3b-2B* was selected for further functional analysis in this study. We subsequently analyzed the expression patterns of *TaSTT3b-2B* in different wheat cultivars. As shown in Figure 1b, at 4 dpi with *R. cerealis*, *TaSTT3b-2B* transcription was higher in the resistant wheat cultivars Shanhongmai and C112633 than in the highly susceptible cultivars Yangmai 158, Zhoumai 18, and Wenmai 6, and the highest expression level was detected in C112633. These results indicate that *TaSTT3b-2B* might play an important role in wheat resistance response to *R. cerealis* infection.

According to the assembled sequence of TraesCS2B02G587900.1, primers were designed to amplify *TaSTT3b-2B* genomic and cDNA sequences from the resistant wheat cultivar C112633. The lengths of genomic and cDNA sequences were 6259 and 2980 bp, respectively. *TaSTT3b-2B* had six exons and it encoded 723 amino acids (Figure 1c). The *TaSTT3b* proteins were

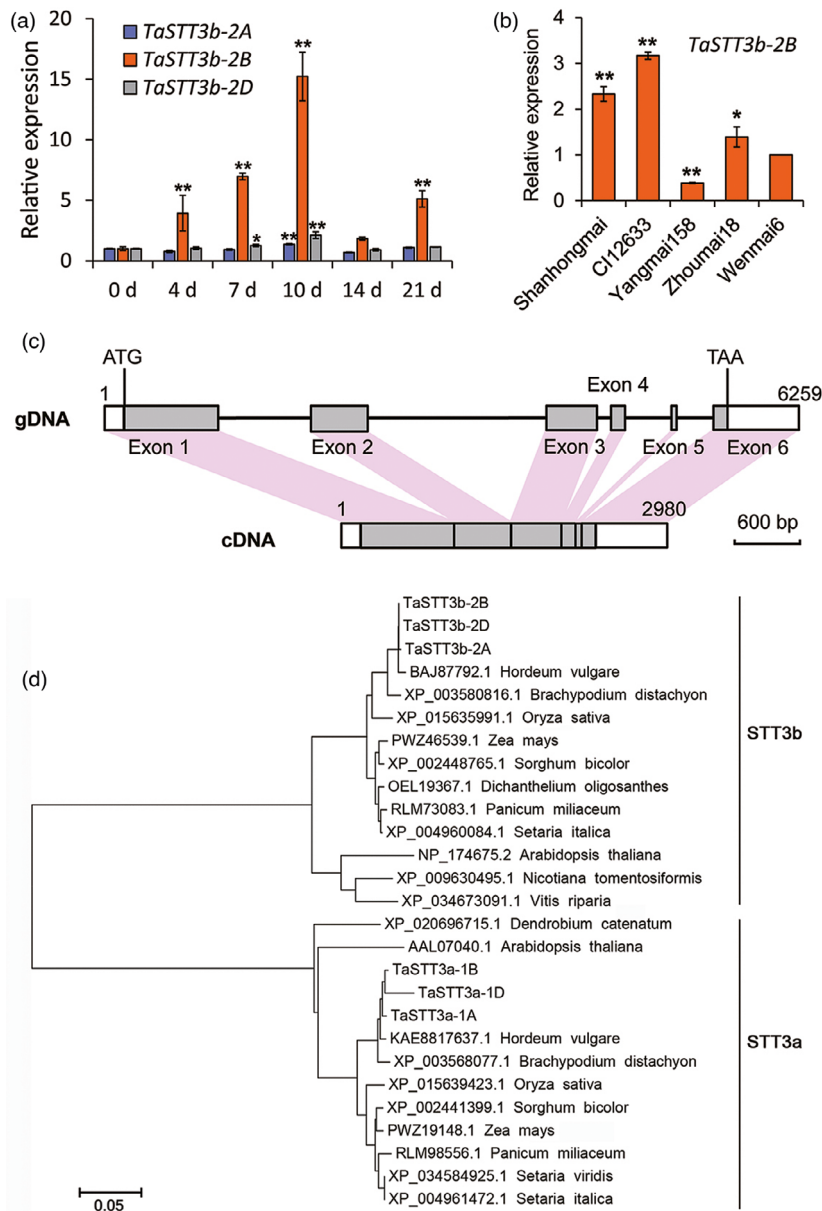


Figure 1 Identification of *TaSTT3b* in wheat. (a) Expression patterns of the three *TaSTT3b* homologs in the wheat line CI12633 at 0, 4, 7, 10, 14, and 21 dpi with *R. cerealis* infection. *TaSTT3b* transcription level in mock-treated plant (0 dpi) was set to 1. (b) Relative transcript levels of *TaSTT3b-2B* in five wheat cultivars at 4 dpi with *R. cerealis* infection. The expression level of *TaSTT3b-2B* in Wenmai6 was set to 1. Data were normalized to wheat *TaActin*. Statistically significant differences are derived from the results of three independent replications (*t*-test: **P* < 0.05, ***P* < 0.01). Bars indicate standard errors of the means. (c) Genomic structure of the *TaSTT3b-2B* gene. Frames and dotted lines represent exons and introns, respectively. (d) Phylogenetic analysis of the TaSTT3a, TaSTT3b, and other STT3 proteins. The phylogenetic tree was constructed from a complete alignment of 26 STT3 protein sequences using the neighbor-joining method with 1000 bootstrap repetitions with the MEGA 6.0 program.

highly conserved with STT3b proteins in Arabidopsis and rice, suggesting that they may be orthologs of TaSTT3b proteins (Figure S2). The genomic sequences of *TaSTT3b-2B* were also obtained from the susceptible wheat cultivar Zhoumai18. Genomic sequence alignment showed that *TaSTT3b-2B* from CI12633 and Zhoumai18 had 98.79% identity, and many single-nucleotide polymorphisms (SNPs) existed (Figure S3).

We summarized *TaSTT3b-2B* and the reported QTLs controlling sharp eyespot resistance on the chromosome 2B (Jiang *et al.*, 2016; Liu *et al.*, 2021; Wu *et al.*, 2017), with their genomic

distributions annotated using the wheat genome database. *TaSTT3b-2B* located on the chromosome 2B was near the SSR marker *Xwmc149* associated with the *Qses.jaas-2B* locus (Figure S4).

To investigate the evolutionary relationships of TaSTT3a and TaSTT3b, a neighbor-joining phylogenetic tree was constructed using ClustalW to align the protein sequences of TaSTT3a and TaSTT3b and their homologs from various plant species. The dendrogram showed that these proteins were clustered into two clades, STT3a and STT3b. Both TaSTT3b and TaSTT3a proteins

were most closely related to their homologs in *Hordeum vulgare* (Figure 1d).

Subcellular localization of the TaSTT3b-2B protein

Prediction of subcellular localization with a transmembrane domain hidden Markov model (TMHMM version 2.0; <http://www.cbs.dtu.dk/services/TMHMM/>) suggested that the TaSTT3b-2B protein was a typical transmembrane protein with 11 transmembrane domains (Figure S5a). To experimentally confirm this prediction, the full-length coding sequence of *TaSTT3b-2B* was fused to the C-terminus of green fluorescent protein (GFP). The GFP-TaSTT3b-2B fusion sequence and an ER marker mCherry-HDEL (Nelson *et al.*, 2007) were coexpressed in wheat mesophyll protoplasts. The results showed that the fluorescence signal of GFP-TaSTT3b-2B could be merged with that of mCherry-HDEL in the ER (Figure S5b), indicating that the TaSTT3b-2B protein localizes to the ER.

Silencing of *TaSTT3a* and *TaSTT3b* genes reduced wheat resistance to *R. cerealis*

To determine the potential functions of *TaSTT3a* and *TaSTT3b* in wheat defense response to *R. cerealis* infection, we generated *TaSTT3a*- and *TaSTT3b*-silenced wheat plants through the barley stripe mosaic virus (BSMV)-based virus-induced gene silencing (VIGS) technique. Two specific fragments of *TaSTT3a-1B* and *TaSTT3b-2B* were amplified to construct two recombinant BSMV vectors, BSMV:TaSTT3a and BSMV:TaSTT3b, respectively (Figure S6). Figure S7a showed the BSMV-VIGS experiment flowchart. Off-target prediction of the *TaSTT3a-1B* VIGS fragment by Si-Fi software indicated efficient siRNA hits of TraesCS1B02G352700.1, TraesCS1D02G342400.1, and TraesCS1A02G340400.1 (Figure S7b), while off-target prediction of the *TaSTT3b-2B* VIGS fragment showed efficient siRNA hits of TraesCS2B02G587900.1, TraesCS2D02G558800.1, and TraesCS2A02G555600.1 (Figure S7c). The prediction analyses suggested efficient silencing of *TaSTT3a* and *TaSTT3b*, and no off-target was predicted for the VIGS construct in wheat. At 10 dpi with BSMV, all C112633 wheat seedlings inoculated with BSMV:GFP (control), BSMV:TaSTT3a, and BSMV:TaSTT3b showed mild chlorotic mosaic symptoms on the fourth leaves, and the expression of the BSMV coat protein (*cp*) gene was clearly detected (Figure 2a and Figure S8a), indicating that the BSMV-VIGS system functioned well. To confirm silencing efficiency, qRT-PCR was used to detect the transcript levels of *TaSTT3a*, as well as *TaSTT3b-2A*, *TaSTT3b-2B*, and *TaSTT3b-2D* in the sheaths of BSMV-infected wheat plants at 7 dpi with *R. cerealis*. As shown in Figure 2b, compared with the control (BSMV:GFP) plants, the transcriptional levels of *TaSTT3b-2A*, *TaSTT3b-2B*, and *TaSTT3b-2D* in the BSMV:TaSTT3b-infected plants were reduced by 74.23%, 90.02%, and 86.26%, respectively. Similarly, in BSMV:TaSTT3a-infected wheat seedlings, the transcriptional level of *TaSTT3a* was reduced by 77.32% (Figure S8b). These results suggest that *TaSTT3a* and *TaSTT3b* were successfully knocked down in BSMV:TaSTT3a- and BSMV:TaSTT3b-infected plants, respectively.

Subsequently, these BSMV-infected wheat plants were inoculated with the *R. cerealis* isolate WK207. At 14 dpi with *R. cerealis* inoculation, the sheaths of BSMV:TaSTT3b-infected C112633 plants displayed more serious necrosis due to sharp eyespot than did BSMV:GFP-infected (control) plants (Figure 2c). The infection types (ITs) of control plants were 0 and 1, while those of 21.88% and 3.13% of the BSMV:TaSTT3b-

infected plants were 2 and 4, respectively (Figure 2d). The average IT value of the BSMV:TaSTT3b-infected plants was 1.13 and was higher than that of BSMV:GFP-treated plants (0.60) at 14 dpi with *R. cerealis* inoculation (Figure 2e). The average area of lesions on TaSTT3b-infected plants was 1.50 cm², whereas the average area on the sheaths of the control plants was smaller at 0.95 cm² 14 days after *R. cerealis* inoculation (Figure 2f). At 28 dpi with *R. cerealis* inoculation, the lesions on the BSMV:TaSTT3b-infected plants were more obvious (Figure 2c). The IT value of 10.00% of BSMV:TaSTT3b-infected plants was 4, and that of 6.67% of BSMV:TaSTT3b-infected plants was 5. No BSMV:GFP-infected plants had an IT value of 4 or 5 (Figure 2d). The average IT value of BSMV:TaSTT3b-infected plants was higher than that of BSMV:GFP-infected plants at 28 dpi with *R. cerealis* inoculation (Figure 2e). The average area of lesions on stems of BSMV:TaSTT3b-infected plants was 1.73 cm², which was significantly higher than that of BSMV:GFP-infected plants (0.68 cm²) at 28 dpi with *R. cerealis* inoculation (Figure 2f). These results indicate that down-regulation of *TaSTT3b* significantly impaired resistance of the wheat cv. C112633 to sharp eyespot, which suggests that *TaSTT3b* is required for host immune response to *R. cerealis* inoculation.

The BSMV:TaSTT3a-infected plants were also inoculated with the *R. cerealis* isolate WK207 (Figure S9a). The ITs of both control and BSMV:TaSTT3a-infected plants were 2, 3, 4, and 5 (Figure S9b). Based on the disease scoring at 28 dpi with *R. cerealis* inoculation, the average area of lesions on stems of BSMV:TaSTT3a-infected plants was 2.99 cm², which was significantly higher than that of BSMV:GFP-infected plants (2.36 cm²) (Figure S9c). However, there was no significant difference between the average IT values of BSMV:TaSTT3a- and BSMV:GFP-infected plants (Figure S9d). The results suggest that compared to TaSTT3b, TaSTT3a plays a minor role in wheat resistance response to the infection of *R. cerealis*.

Overexpression of *TaSTT3b-2B* boosted wheat resistance to *R. cerealis*

To further investigate potential functions of TaSTT3b in wheat defense response to *R. cerealis*, we constructed an overexpression vector pWMB-TaSTT3b-2B-His (Figure S10) and transformed this construct into a hexaploid wheat cv. Zhoumai 18, generating *TaSTT3b-2B* transgenic wheat lines. In total, 55 wheat regeneration seedlings were obtained. Based on PCR detection, 14 T₀ transgenic positive plants were verified (Figure S11), among which three lines (OX49, OX74, and OX89) were selected for further study and functional/phenotypic identification (Figure 3a). The droplet digital PCR (ddPCR) was used to measure *TaSTT3b-2B* transgene copy number in the transgenic wheat lines. Meanwhile, *PINb-D1b* (*Puroindoline-b D1b*) was used as the reference with two copies in hexaploid wheat (Collier *et al.*, 2017). The ddPCR results showed that the transgenic lines OX49 and OX74 contained two copies of introduced *Ubi-TaSTT3b-2B-Tnos* chimera, respectively, and OX89 carried three copies (Figure 3b, Figure S12). The expression levels of *TaSTT3b-2B* transgene individuals from the T₁–T₃ generations of the OX49, OX74, and OX89 lines were detected using qRT-PCR. As shown in Figure 3c, the transcriptional levels of *TaSTT3b-2B* in these three transgenic lines were significantly higher than those in the un-transformed (wild type, WT) Zhoumai18, indicating the introduced *TaSTT3b-2B* was overexpressed in these three lines. Western blotting

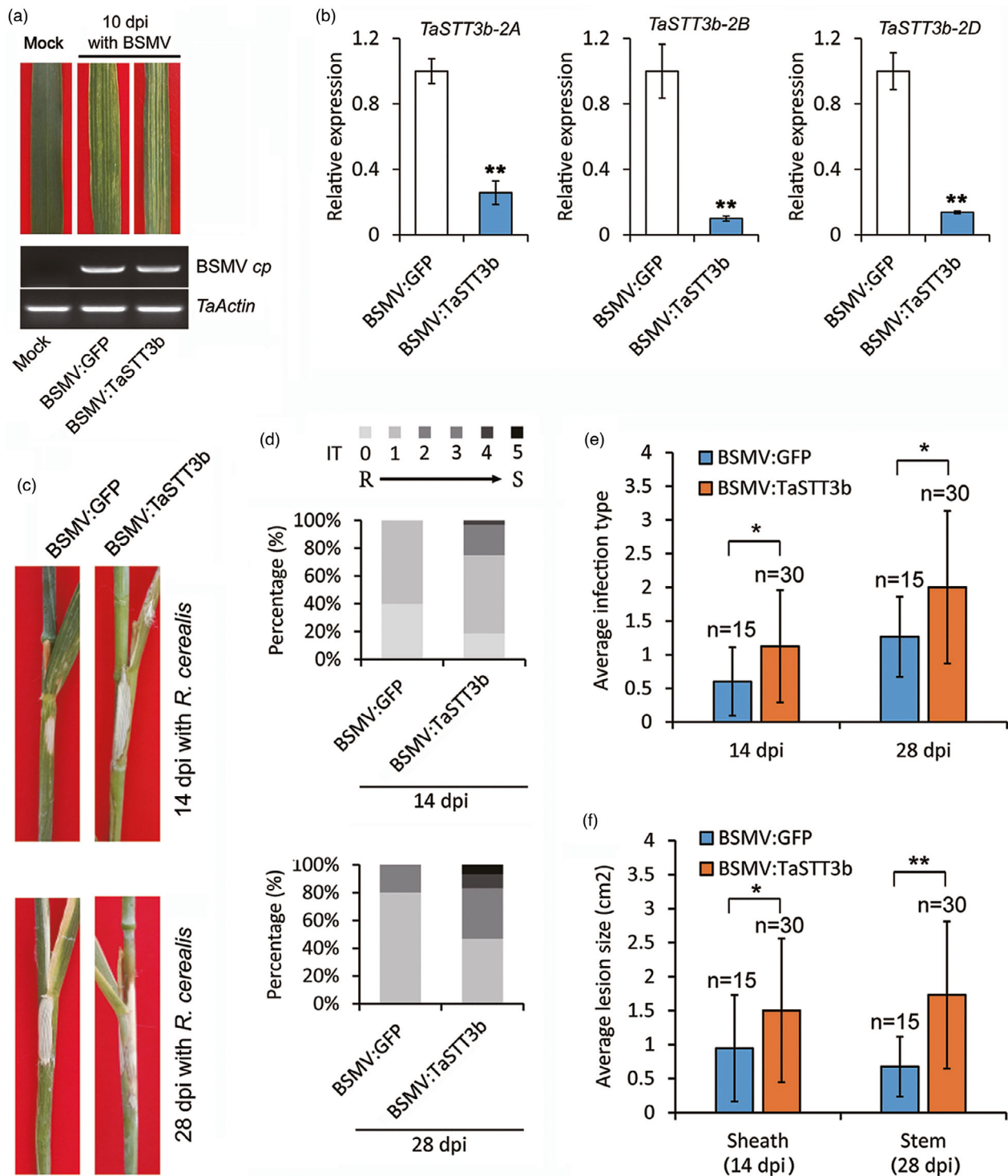


Figure 2 Barley stripe mosaic virus (BSMV)-induced *TaSTT3b*-silencing impairs resistance of wheat CI12633 to *Rhizoctonia cerealis*. (a) Mild chlorotic mosaic symptoms on leaves of CI12633 plants infected by BSMV:GFP or BSMV:TaSTT3b for 10 days. Detection of the BSMV coat protein (*cp*) gene was detected by RT-PCR. (b) Relative transcriptional levels of the three *TaSTT3b* homologs (*TaSTT3b-2A*, *TaSTT3b-2B*, and *TaSTT3b-2D*) in BSMV:GFP- and BSMV:TaSTT3b-infected wheat plants by qRT-PCR analysis. The relative transcriptional levels of *TaSTT3b* homologs in BSMV:TaSTT3b-infected CI12633 plants is relative to those in BSMV:GFP-infected plants (set to 1). (c) Sharp eyespot symptoms on CI12633 plants infected with BSMV:GFP and BSMV:TaSTT3b at 14 and 28 dpi with *R. cerealis* infection. (d) Percentages of BSMV:GFP- and BSMV:TaSTT3b-infected CI12633 plants with different sharp eyespot infection types (ITs) at 14 and 28 dpi with *R. cerealis* infection. (e) Average ITs of BSMV:GFP- and BSMV:TaSTT3b-infected CI12633 plants at 14 and 28 dpi with *R. cerealis* infection. (f) Average size of lesions in BSMV:GFP- and BSMV:TaSTT3b-infected CI12633 plants at 14 and 28 dpi with *R. cerealis* infection. Bars indicate standard errors of the means (*n* varies for each column and is shown in each case directly on the graphs). Single and double asterisks represent significant differences between BSMV:GFP- and BSMV:TaSTT3b-infected CI12633 plants determined by Student's *t*-test at $P < 0.05$ and $P < 0.01$, respectively.

analysis revealed that the introduced TaSTT3b-2B-His fusion protein constitutively accumulated in these transgenic wheat lines (Figure 3d).

Because the resistance/susceptibility of wheat to *R. cerealis* is easily influenced by environmental conditions, we tested the resistance of transgenic and WT wheat plants to *R. cerealis* in Beijing and Nanjing in 2018, 2019, and 2020. The three *TaSTT3b-2B* overexpressing wheat lines, OX49, OX74, and OX89, displayed significantly enhanced resistance to sharp eyespot caused by *R. cerealis* (Figure 3e). Mean disease index values of the WT Zhoumai18, 76.96 (2018) and 39.46 (2019), were greater than mean disease index values of the three

transgenic lines, 38.50–59.73 (2018) and 28.99–32.89 (2019), in Beijing (Figure 3f, g). Compared with the WT Zhoumai18, the three transgenic lines also displayed markedly elevated resistance to sharp eyespot in plants grown in Nanjing. For example, the disease index values of three overexpressing lines OX49, OX74, and OX89 were separately 21.16, 21.73, and 22.80 in 2019, and 37.07, 36.49, and 36.76 in 2020, respectively, and they were all lower than those of the WT Zhoumai18 (Figure 3h,i). These results indicate that *TaSTT3b-2B* overexpression improved resistance of the transgenic wheat to sharp eyespot, and TaSTT3b-2B positively participates in wheat resistance to *R. cerealis* infection.

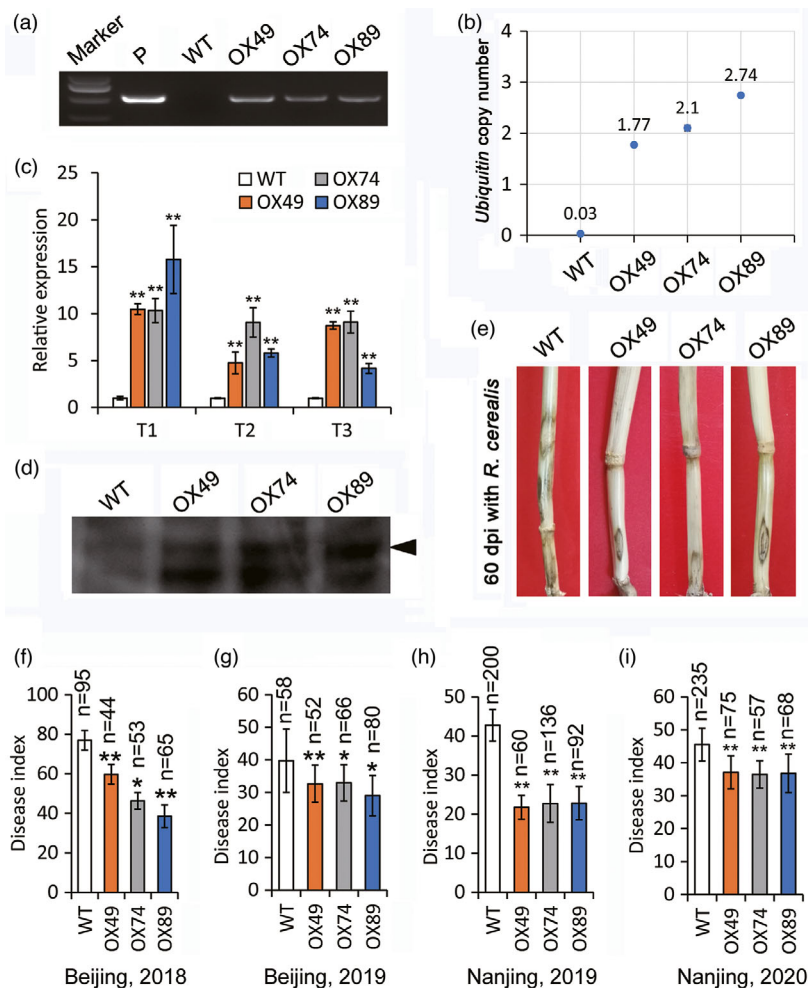


Figure 3 Molecular characterizations of *TaSTT3b-2B* overexpressing wheat plants and plant responses to *Rhizoctonia cerealis* infection. (a) PCR patterns of three *TaSTT3b-2B* transgenic lines (OX49, OX74, and OX89) and wild-type (WT) wheat Zhoumai18 using the primers specific to the *TaSTT3b-2B-Tnos* cassette. Marker, DL2, 000 DNA marker; P, the transformation vector pWMB122-*TaSTT3b-2B* as the positive control. (b) Transgene copy number measurements in *TaSTT3b-2B* transgenic and WT lines. Primers and probes were designed to detect the sequence of the maize *Ubi* promoter, which was used to control *TaSTT3b-2B* expression. (c) qRT-PCR analyses of the relative transcriptional levels of *TaSTT3b-2B* in *TaSTT3b-2B* transgenic lines in the T₁–T₃ generations. Mean values of *TaSTT3b-2B* in WT Zhoumai18 were defined as 1. Three biological replicates per line were averaged (*t*-test; ***P* < 0.01). Bars indicate standard errors of the means. (d) Western blot pattern of the three *TaSTT3b-2B* overexpressing lines and WT Zhoumai18 using an anti-6×His antibody. Similar results were obtained from three independent replicates. (e) Typical symptoms of sharp eyespot in the three *TaSTT3b-2B* overexpressing and WT Zhoumai18 lines at 60 dpi with *R. cerealis* infection. (f–i) Disease index of *TaSTT3b-2B* overexpressing and WT Zhoumai18 lines. The phenotypes were identified in wheat grown in Beijing in 2018 and 2019, as well as in Nanjing in 2019 and 2020. Bars indicate standard errors of the means (*n* varies for each column and is shown in each case directly on the graphs), and asterisks indicate significant differences between WT and transgenic lines using Student's *t*-tests (*, *P* < 0.05; **, *P* < 0.01).

RNA-seq analysis identifies defense-related genes modulated by *TaSTT3b-2B*

To further dissect the molecular basis of *TaSTT3b-2B*-mediated wheat defense response to *R. cerealis*, we performed RNA-seq analysis on *TaSTT3b-2B* overexpressing and WT Zhoumai18 plants at 4 dpi with *R. cerealis* inoculation (Table S2). A total of 2264 differentially expressed genes (DEGs) were obtained based on the criteria of a fold change of 2 and false discovery rate (FDR) < 0.05. Among them, 1751 genes were highly expressed in *TaSTT3b-2B* overexpressing wheat lines in comparison to the WT, and 513 genes were expressed at a lower level (Figure S13, Table S3). Gene Ontology (GO) analysis of the DEGs indicated that *TaSTT3b-2B* overexpression affected multiple processes in the transgenic wheat plants. Notably, some of the DEGs were clustered into stress response-related terms such as 'response to stimulus', 'signaling', and 'immune system process' (Figure S14), suggesting that overexpression of *TaSTT3b-2B* affected the expression levels of genes involved in stress and immune responses. The genes for diverse processes were also enriched, which includes metabolic, cellular, and single organism processes, implying that the *TaSTT3b-2B*-mediated defense response to *R. cerealis* infection might be a consequence of multiple biological processes in wheat (Figure S14).

As shown in Figure 4a, 297 of the DEGs were categorized for their involvement in defense response to pathogens based on GO analysis, Pfam annotation, and SWISS PROT annotation (Table S4). These genes encoded cytochrome P450; GDSL-like lipase (GLIP); O-methyltransferase; ABC transporter; pathogenesis-related protein; protein kinase; oxygenase; 1,3-beta-glucosidase; lipoxygenase (LOX); chitinase; and some transcription factors (TFs), such as WRKY TFs, basic helix-loop-helix TFs, myeloblastosis-related (MYB) TFs, ethylene-responsive factors (ERFs), MADS-box TFs, basic leucine zipper (bZIP) TFs, and GATA TFs. It is worth mentioning that 27 GLIP genes were identified in the DEGs, 26 of which were significantly up-regulated in *TaSTT3b-2B* overexpressing lines (Figure S15). To verify the reliability of the RNA-seq data, eight defense-related genes, including *TaBRI1* (BRASSINOSTEROID INSENSITIVE 1, TraesCS3B02G551200), *TaCOMT* (caffeic acid O-methyltransferase, TraesCS3B02G612000), *TaLTP* (lipid transfer protein, TraesCS2B02G501000), *TaGlu1* (glucosidase, TraesCS2B02G600200), *TaMAH1* (midchain alkane hydroxylase, TraesCSU02G101400), *TaGLIP1* (TraesCS4A02G397000), *TaLOX* (TraesCS5B02G382600), and *TaAOS2* (allene oxide synthase 2, TraesCS4A02G061800), were chosen to be validated by qRT-PCR. As shown in Figure 4b, the relative transcript levels of these eight genes in *TaSTT3b-2B* overexpressing plants were significantly higher than those of the WT plants. Because of being generally consistent with the RNA-seq data, these results suggested that the RNA-seq data should be reliable. Expectedly, the transcriptional levels of these defense-related genes were significantly down-regulated in the *TaSTT3b*-silenced wheat plants in comparison with the BSMV:GFP-infected (control) wheat plants (Figure S16). These results indicated that these eight defense-related genes were regulated by *TaSTT3b-2B* and were possibly downstream of *TaSTT3b-2B*.

Overexpression of *TaSTT3b-2B* increased grain size in transgenic wheat with *R. cerealis* infection

To explore if overexpression of *TaSTT3b-2B* influences yield-affected factors, spike number per m², spike length, spikelet

number per spike, grain number per spike, grain length, grain width, and thousand-grain weight (TGW) were examined in both *TaSTT3b-2B* transgenic and WT plants infected with *R. cerealis*. Notably, there was a significant difference in grain size (grain length and grain width) between *TaSTT3b-2B* overexpressing wheat lines and the WT Zhoumai18 line. The overexpressing wheat lines produced bigger kernels than the WT Zhoumai18 line (Figure 5a). The grain length (Figure 5b), grain width (Figure 5c), and TGW (Figure 5d) all were significantly higher in these three *TaSTT3b-2B* overexpressing wheat lines (OX49, OX74, and OX89) than those in the WT Zhoumai18 plants. In contrast, there were no significant differences in spike number per m², spike length, spikelet number per spike, and grain number per spike between *TaSTT3b-2B* overexpressing wheat lines and the WT Zhoumai18 line (Figure S17).

To investigate the relationship between *TaSTT3b-2B* expression and grain size, we analyzed the expression profile of *TaSTT3b-2B* in wheat varieties with different TGWs. As shown in Figure 5e and 5f, the expression level of *TaSTT3b-2B* was higher in wheat varieties with higher TGW (40–50 g) than in those with low TGW (<40 g), and these varieties with the highest TGW (>50 g) showed the highest expression level of *TaSTT3b-2B*. These data suggested that the expression level of *TaSTT3b-2B* was positively associated with the grain size in wheat and support the abovementioned results, that is, greater grain weight of the *TaSTT3b-2B* overexpressing wheat.

The high molecular weight glutenin (HMW-GS), starch synthase, starch branching enzyme, and sucrose synthase have shown significant associations with grain size in wheat or rice (Daba *et al.*, 2018; Jiang *et al.*, 2011; Li *et al.*, 2011). In order to explore the mechanisms underlying the increased grain weight of the *TaSTT3b-2B* overexpression, we examined relative transcript abundances of *TaSSIIa* (encoding starch synthase IIa), *TaSBEIIb* (encoding starch branching enzyme IIb), the HMW-GS genes [*TaGlu1-1B1* (TraesCS1B02G329992), *TaGlu1-1B2* (TraesCS1B02G329711), *TaGlu1-1D1* (TraesCS1D02G317301), *TaGlu1-1D2* (TraesCS1D02G317211), and *TaGlu-4A* (TraesCS4A02G485400)], the sucrose synthase genes, including *TaSuSy1* (TraesCS7D02G159800), *TaSuS-2A* (TraesCS2A02G168200), *TaSuS-2B* (TraesCS2B02G194200), and *TaSuS-2D* (TraesCS2D02G175600), and the grain size gene *TaGS5* (TraesCS6B02G261700, a wheat homologous gene of rice *GS5*) in *TaSTT3b-2B* overexpressing and WT wheat lines. The qRT-PCR analyses showed that the expression levels of these grain size-related genes were markedly up-regulated in *TaSTT3b-2B* overexpressing wheat lines compared to those in the WT Zhoumai18 line (Figure 5g). These data suggest that overexpression of *TaSTT3b-2B* increased grain weight by up-regulating the expression of these grain size-related genes. Interestingly, treatment with exogenous JA increased the transcript levels of these grain size-related genes except of those of *TaGlu1* (Figure 5h), implying that JA biosynthesis might contribute to grain size in wheat.

TaSTT3b-2B-mediated resistance to *R. cerealis* possibly through the JA signal pathway

JA is a crucial signal molecule in plant resistance against pathogens, especially in resistance to necrotrophic pathogens (Pieterse *et al.*, 2009). Thus, we endeavored to investigate whether overexpression of *TaSTT3b-2B* alters the defense response of wheat to *R. cerealis* through the JA signal pathway.

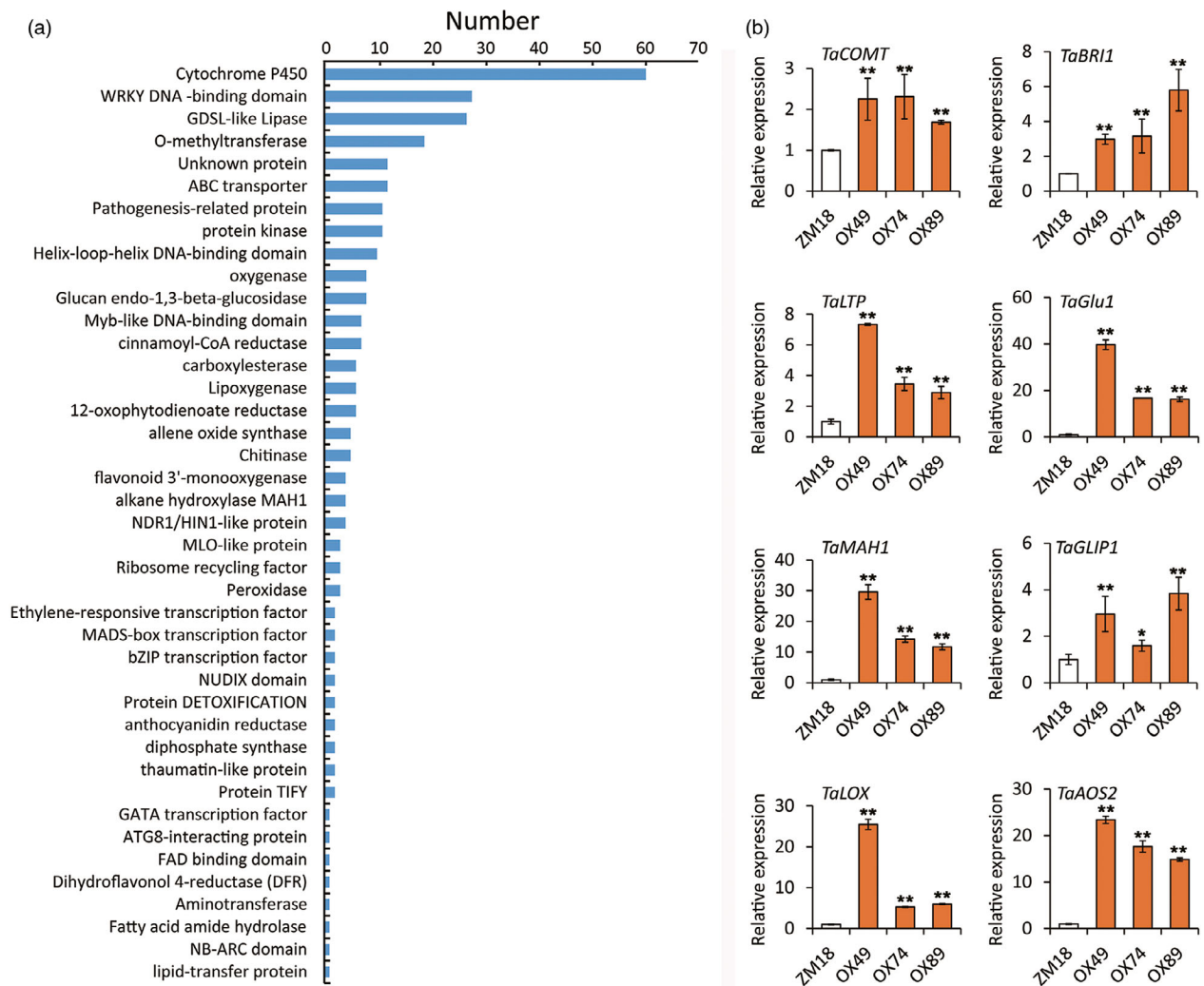


Figure 4 Defense-related genes regulated by TaSTT3b-2B. (a) Distribution of defense-related genes in differentially expressed genes (DEGs). (b) RT-qPCR analysis of *TaCOMT*, *TaBRI1*, *TaLTP*, *TaGlu1*, *TaMAH1*, *TaGLIP1*, *TaLOX*, and *TaAOS2* expression in three *TaSTT3b-2B* transgenic lines (OX49, OX74, and OX89) and WT Zhoumai18 at 4 dpi with *Rhizoctonia cerealis* infection. qRT-PCR data were normalized to wheat *TaActin*. The data from three replicates are shown with \pm SD. The single and double asterisks represent significant differences determined by Student's *t*-test at $P < 0.05$ and $P < 0.01$, respectively.

The expression profile of *TaSTT3b-2B* in wheat response to exogenous JA was detected. As shown in Figure 6a, the expression of *TaSTT3b-2B* was significantly induced from 1 to 8 hours post treatment with JA.

The JA pathway, including JA biosynthesis and the subsequent JA signal transduction, has been characterized (Lyons *et al.*, 2013). In the DEGs identified in this study, 30 JA biosynthesis-related genes, comprising 21 *lipoxygenase* (*LOX*) genes, five *allene oxide synthase* (*AOS*) genes, and four *OPDA reductase* (*OPR*) genes, were identified (Figure 6b, Table S5). With the exceptions of two *OPR* genes (TraesCS1D02G013600 and TraesCS1A02G015800), the transcript abundances of the other 28 JA-related genes were significantly higher in *TaSTT3b-2B* overexpressing wheat plants than those in the WT plants based on a log₂ fold-change analysis (Figure 6b, Table S5). Accordingly, compared to the WT line, high accumulation of JA was observed in the *TaSTT3b-2B* transgenic lines (Figure 6c). These results suggested that TaSTT3b-2B positively regulated JA biosynthesis in wheat.

As shown in Figure 6c, *R. cerealis* infection induced JA biosynthesis, and the transgenic wheat lines still had a higher level of JA content than the WT plants. Seven JA biosynthesis-related genes, *TaLOX-5A*, *TaLOX-5D*, *TaLOX-6D*, *TaAOS-4A*, *TaAOS-4D*, *TaOPR-1D*, and *TaOPR-4B*, were chosen for further gene expression analysis in wheat after infection by *R. cerealis*. The expression levels of these seven genes were significantly induced by *R. cerealis* infection (Figure 6d). These data indicated that TaSTT3b-2B positively regulated the transcripts of these JA biosynthesis-related genes, which were also induced by *R. cerealis* infection.

To further explore the relationship between the TaSTT3b-2B-mediated resistance and the JA biosynthesis, we first examined the transcriptional levels of two JA-related genes, *TaLOX* and *TaOPR*, in TaSTT3b-silenced and BSMV:GFP-infected wheat plants. The data showed that silencing of *TaSTT3b-2B* down-regulated the transcriptional levels of *TaLOX* and *TaOPR* (Figure 7a). Next, TaSTT3b-silenced and BSMV:GFP-infected wheat plants were pretreated with MeJA and then inoculated

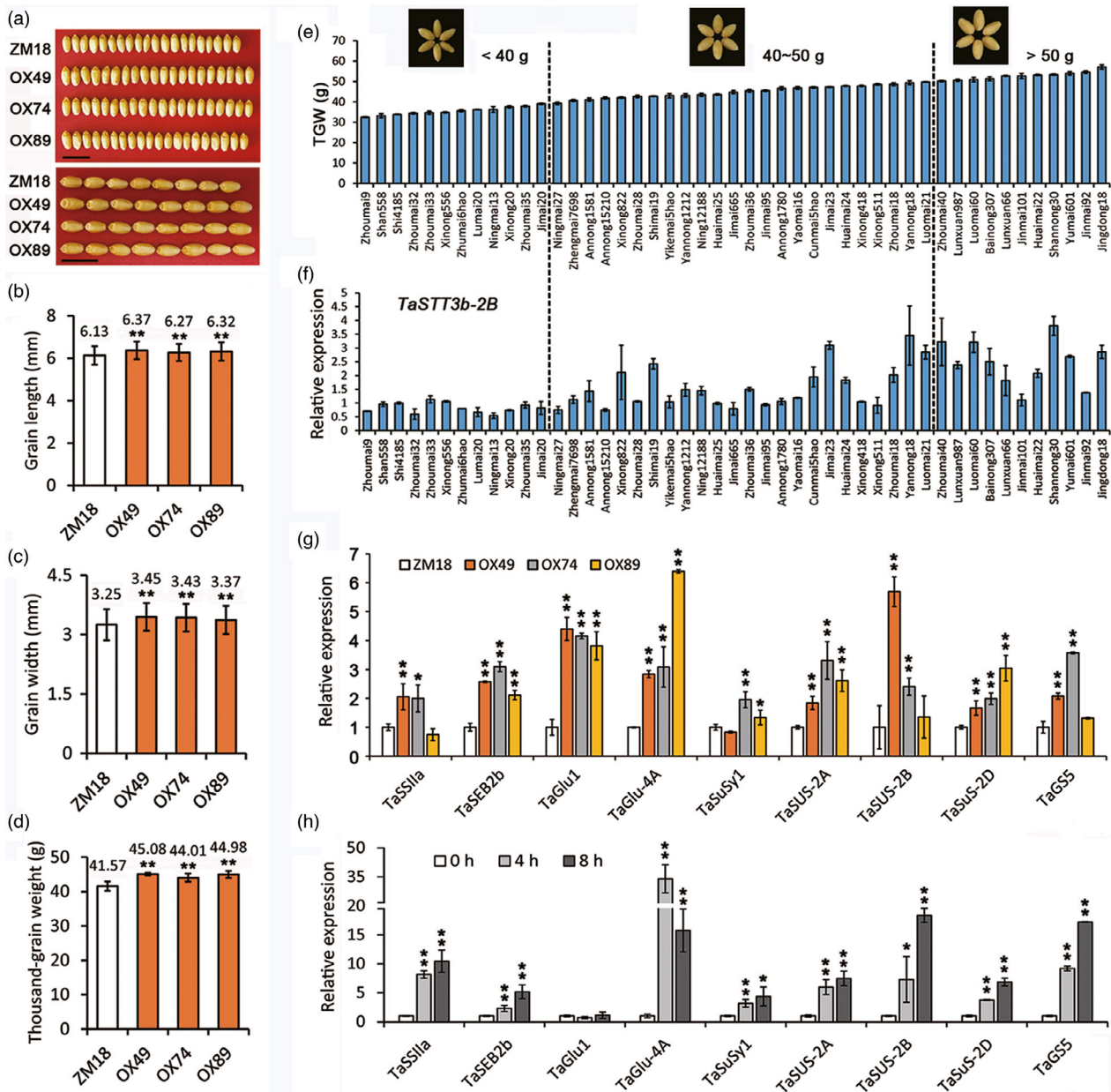


Figure 5 *TaSTT3b-2B* regulates grain size in transgenic wheat infected by *Rhizoctonia cerealis*. (a) Grains of *TaSTT3b-2B*-overexpressing and WT Zhoumai18 lines. Scale bar = 1 cm. (b–d) Grain size-related phenotypes of *TaSTT3b-2B*-overexpressing and WT Zhoumai18 lines: grain length (b), grain width (c), and TGW (thousand-grain weight) (d). (e) TGW of different wheat varieties. Three replicates were used, each with approximately 20 g grains. (f) Expression levels of *TaSTT3b-2B* in different wheat varieties. (g) qRT-PCR analysis of *TaSSIIa*, *TaSBEIIb*, *TaGlu1*, *TaGlu-4A*, *TaSuSy1*, *TaSuS-2A*, *TaSuS-2B*, *TaSuS-2D*, and *TaGS5* in three *TaSTT3b-2B* transgenic lines (OX49, OX74, and OX89) and WT Zhoumai18. (h) Expression patterns of these grain size-related genes in wheat response to exogenous JA. Wheat plants at the four-leaf stage were sprayed with 0.1 mM MeJA. qRT-PCR data were normalized to wheat *TaActin*. The data from three replicates are shown with \pm SD. The single and double asterisks represent significant differences determined by Student's *t*-test at $P < 0.05$ and $P < 0.01$, respectively.

with *R. cerealis*. Compared with the mock group given 0.1% Tween-20, MeJA pretreatment increased wheat resistance to *R. cerealis*, and there was no significant difference in the observed disease symptoms between *TaSTT3b*-silenced and BSMV:GFP-infected plants (Figure 7b). Accordingly, the expression level of *R. cerealis actin* mRNA (*RcActin*), used as a measure of fungal biomass in the pathogen-inoculated wheat, was consistent with the symptoms of these plants (Figure 7c). Furthermore, JA treatment elevated the transcriptional levels of some defense-

related genes, including *TaCOMT*, *TaBRI1*, *TaLTP*, *TaGlu*, *TaMAH1*, *TaGLIP1*, *TaLOX*, and *TaAOS2* (Figure S18). In contrast, pretreatment with the JA biosynthesis inhibitor DIECA attenuated the *TaSTT3b-2B*-mediated resistance to *R. cerealis* (Figure 7d), and the detection of the *RcActin* expression level supported the altered disease symptoms described above (Figure 7e). Overall, these results suggest that *TaSTT3b-2B*-mediated resistance to *R. cerealis* was partially dependent on JA biosynthesis.

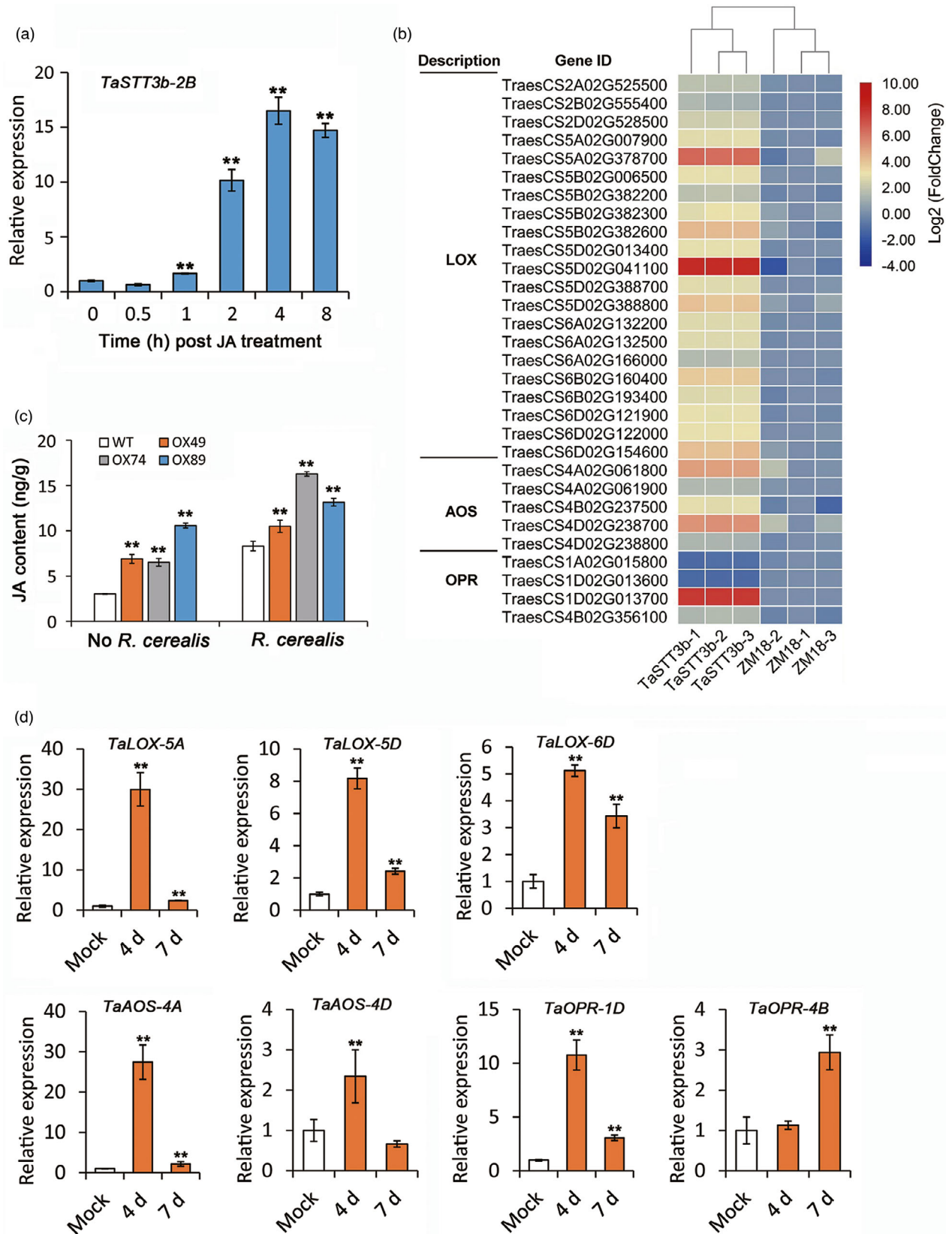


Figure 6 TaSTT3b-2B-mediated resistance to *Rhizoctonia cerealis* is associated with the JA biosynthesis. (a) Expression patterns of *TaSTT3b-2B* in leaves of Zhoumai18 wheat in response to applications of exogenous JA. Wheat plants at the four-leaf stage were sprayed with 0.1 mM MeJA. (b) JA biosynthesis-related genes in differentially expressed genes (DEGs). These genes were identified by transcriptome analysis as DEGs identified between *TaSTT3b-2B* overexpressing and WT Zhoumai18 plants (based on log2 fold change). TaSTT3b-1, TaSTT3b-2, and TaSTT3b-3 indicate samples of three *TaSTT3b-2B* overexpressing lines. ZM18-1, ZM18-2, and M18-3 indicate three leaf sheath samples of the WT Zhoumai18 line. (c) JA contents of *TaSTT3b-2B* overexpressing and WT Zhoumai18 plants before and after *R. cerealis* infection for 4 days. (d) Expression patterns of JA-related genes in wheat response to *R. cerealis* infection for 4 and 7 days. Data were normalized to wheat *TaActin*. Statistically significant differences were derived from the results of three independent replications (Student's *t*-test: **P* < 0.05, ***P* < 0.01). Bars indicate standard errors of the means.

Discussion

The majority of the reports on STT3 subunits mainly focus on involvement of STT3a in plant resistance to abiotic (Jeong *et al.*, 2018; Koiwa *et al.*, 2003) and biotic (Häweker *et al.*, 2010; Jia *et al.*, 2020; de Oliveira *et al.*, 2016; Zhang *et al.*, 2015) stresses. For instance, cell wall biosynthesis was abnormal in *Arabidopsis*

stt3a mutants, which led to compromised salt tolerance (Koiwa *et al.*, 2003). STT3a has also been shown to play a key role in BAK1-/SERK4-regulated cell death (de Oliveira *et al.*, 2016). However, no study of STT3b involved in plant immunity to various pathogens has been reported. In this study, two OST subunit genes, *TaSTT3a* and *TaSTT3b*, were identified from wheat. The qRT-PCR analysis showed that *TaSTT3b-2B* expression, but not

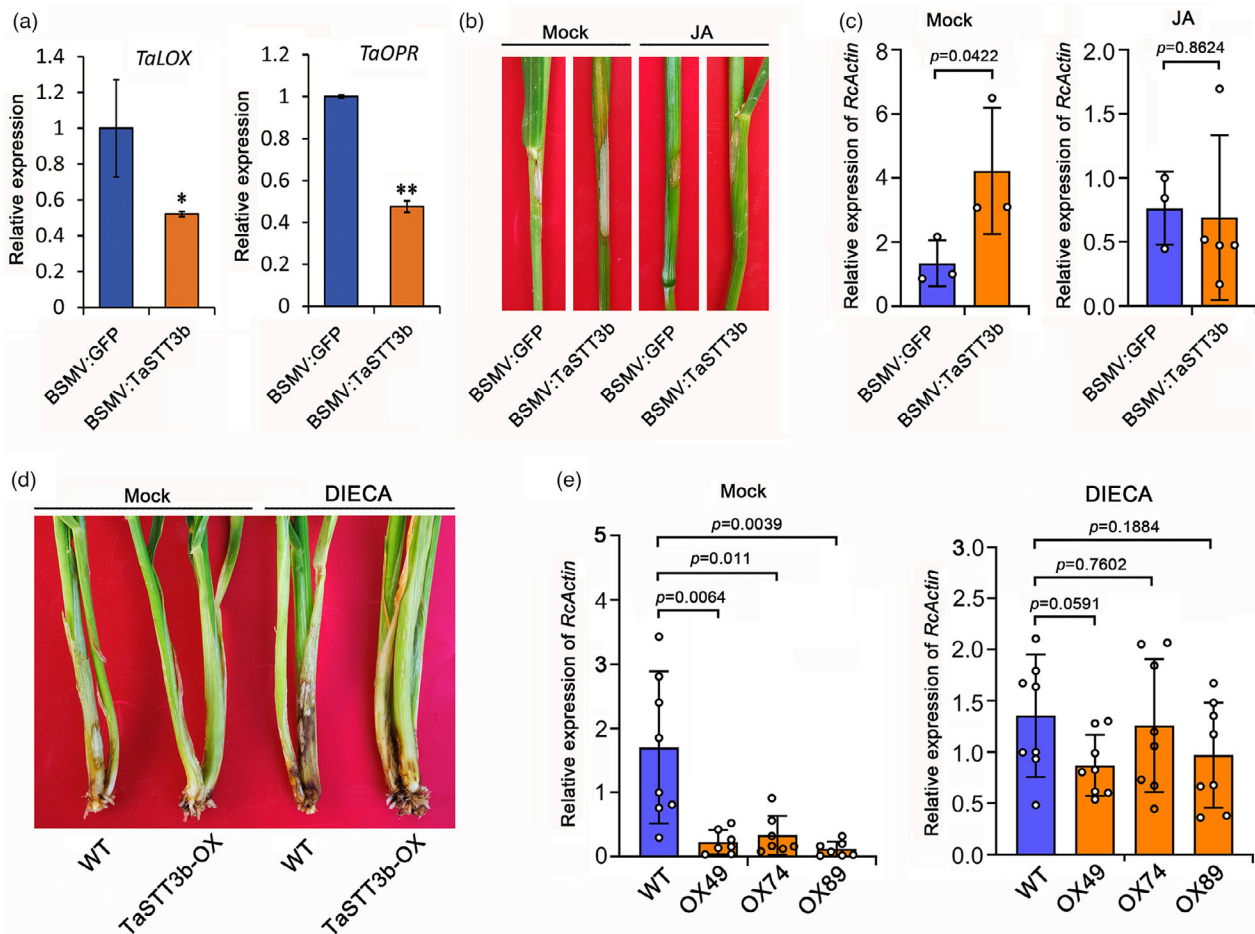


Figure 7 Jasmonic acid positively regulates TaSTT3b-2B-mediated resistance to *Rhizoctonia cerealis*. (a) Expression levels of *TaLOX* and *TaOPR* in *TaSTT3b-2B*-silenced wheat plants. The expression levels of target genes in BSMV:GFP-infected plants were set to 1. Data were normalized to wheat *TaActin*. (b) Sharp eyespot symptoms of *TaSTT3b-2B*-silenced and BSMV:GFP-infected plants after treatment with exogenous JA. C112633 plants at 20 dpi with BSMV:GFP or BSMV:TaSTT3b were sprayed with 0.1 mM MeJA and 0.1% Tween-20 (mock). (c) qRT-PCR analysis of the *R. cerealis actin* (*RcActin*) gene in leaf sheaths of *TaSTT3b-2B*-silenced and control C112633 plants after JA or mock treatment. (d) Sharp eyespot symptoms of *TaSTT3b-2B* overexpressing and WT plants after pretreatment with the JA biosynthesis inhibitor DIECA. Seedlings sprayed with 0.1% Tween-20 were used as mock. (e) qRT-PCR analysis of the *RcActin* gene in leaf sheaths of *TaSTT3b-2B* overexpressing and WT plants after DIECA or mock treatment. The expression level represents the biomass of *R. cerealis*. Statistically significant differences were derived from the results of three independent replications (Student's *t*-test: **P* < 0.05, ***P* < 0.01). Bars indicate standard errors of the means.

TaSTT3a, was markedly induced by *R. cerealis* infection, and *TaSTT3b-2B* produced significantly higher transcriptional levels in *R. cerealis*-resistant wheat genotypes than in the susceptible wheat genotypes. The functional dissection data indicate that *TaSTT3b-2B*, acting as a positive regulator, was required for wheat resistance response to *R. cerealis*. To our knowledge, this is probably the first investigation to uncover the positive regulation of *STT3b* in plant resistance responses to necrotrophic fungal pathogens. This study undoubtedly deepens understanding of biological functions of the *STT3* subunit in plant species.

To explore the molecular mechanism underlying the defensive role of *TaSTT3b-2B*, RNA-seq-based transcriptomic analyses were deployed to identify a number of defense-associated genes, being differently expressed between *TaSTT3b-2B* overexpressing and WT wheat lines. In addition to MYB, ERF, GATA, COMT, chitinase, pathogenesis-related (PR) protein, and 1,3-beta-glucosidase that have been reported to be involved in the wheat defense response to *R. cerealis* infection (Liu et al., 2009, 2020; Wang et al., 2018; Wei et al., 2016; Zhang et al., 2007; Zhu et al., 2014, 2018), some other types of genes, such as those coding the cytochrome P450 enzyme, GLIP, LOX, and AOS, were also identified. The qRT-PCR assay results on eight defense-related genes in *TaSTT3b-2B*-silenced and overexpressing plants, as well as the control wheat plants, supported that the RNA-seq data were reliable. These data suggest that *TaSTT3b-2B* expression is required for the expression of these defense-related genes during wheat resistance to *R. cerealis* infection. Thus, overexpressing *TaSTT3b-2B* increased the expression of these defense-related genes, resulting in enhanced resistance of the transgenic wheat to *R. cerealis*.

JA is an essential plant hormone that regulates certain types of disease resistance, especially resistance to necrotrophic pathogens (Bari and Jones, 2009; Peng et al., 2012). In plants, increasing evidence has shown that JA is able to induce the expression of certain defense-related genes (Liu et al., 2020; McGrath et al., 2005; Peng et al., 2012; Pieterse et al., 2009; Thomma et al., 1998). For example, an increase in endogenous JA and the expression of JA synthesis-related genes *LOX*, *AOS2*, and a subset of PR genes, such as *PR3* and *PR10*, conferred enhanced resistance to sheath blight and blast fungi in *WRKY30* overexpression rice (Peng et al., 2012). Both *WRKY4* and *WRKY80* have been found to enhance rice resistance to sheath blight by inducing the up-regulated expression of JA- and ET-responsive PR genes (Peng et al., 2016). In this study, transcriptional abundance of *TaSTT3b-2B* was induced by *R. cerealis* and JA treatments, and higher accumulation of JA was observed in the resistant *TaSTT3b-2B* overexpressing wheat lines than that of the WT wheat line, suggesting that the *TaSTT3b-2B*-mediated resistance to *R. cerealis* infection was positively associated with JA biosynthesis/signaling. Consistently, *TaSTT3b-2B* positively promoted JA synthesis by positively regulating the expression of the JA synthesis-related genes *TaLOX-5A*, *TaLOX-5D*, *TaLOX-6D*, *TaAOS-4A*, and *TaAOS-4D*, whose transcripts were also responsive to *R. cerealis* infection. Importantly, exogenous JA application could counteract the reduced resistance of *TaSTT3b-2B*-silenced wheat plants to *R. cerealis*, and the JA also induced expression of the *TaSTT3b-2B*-regulated defense-related genes. Similarly, in rice, application of exogenous JA induced resistance to *R. solani* (Taheri and Tarighi, 2010) and *M. oryzae* (Riemann et al., 2013). Meanwhile, pretreatment with DIECA, an inhibitor of JA synthesis, reduced the *TaSTT3b-2B*-mediated resistance to *R. cerealis*. Taken together, these data suggest that JA biosynthesis might play an

important role in *TaSTT3b-2B*-mediated immune response to *R. cerealis*. Our study not only showed the positive regulatory function of *TaSTT3b-2B* in the expression of JA biosynthesis-related genes but also demonstrated the importance of JA treatment in expression of *TaSTT3b-2B*-mediated defense-related genes and disease resistance in wheat.

Grain weight, grain number per spike, and spike number per plant are the most important traits in relation to achieving greater grain yield per plant. In this study, analyses of the agronomic traits and yield parameters showed that the *TaSTT3b-2B* overexpressing wheat lines possessed greater grain length and width and higher TGW than those possessed by WT after both groups were infected by *R. cerealis*. Starch and sucrose synthases have been shown to contribute to grain yield (Fan et al., 2019; Hou et al., 2014; Xie et al., 2018). In maize, overexpression of mutated *ZmDA1* or *ZmDAR1* improved kernel yield by promoting starch synthesis (Xie et al., 2018). In rice, overexpression of a sucrose synthase gene, *OsSUS3*, significantly improved grain weight by dynamically regulating cell division and starch accumulation (Fan et al., 2019). In wheat, the sucrose synthase genes *TaSuS1* and *TaSuS2* showed significant association with grain yield (Hou et al., 2014; Daba et al., 2018). Here, the results showed that the transcriptional levels of two starch synthase-related genes, *TaSSIIa* and *TaSBEIIb*, and four sucrose synthase genes, *TaSuS1y*, *TaSuS-2A*, *TaSuS-2B*, and *TaSuS-2D*, were higher in *TaSTT3b-2B* overexpressing plants than in WT plants. These data indicate that *TaSTT3b-2B* promoted grain weight most possibly by affecting the expression of starch synthase and sucrose synthase genes. In a most recent article, in wheat, mutation of the JA synthetic gene, *KAT-2B*, produces smaller grains and accumulates less JA, while overexpression of *KAT-2B* increases grain weight and yield in plants grown in field trials (Chen et al., 2020). Rice mutants defective in JA biosynthesis (*dfo2* and *Osopr7*) or signaling (*Osmyc2*) exhibited various degrees of abnormality in spikelet development, including abnormal number or morphology of lemma, palea, glume, lodicule, and floral organs, which can be partially rescued by application of exogenous JA (You et al., 2019). The TCP (Teosinte branched/Cycloideae/PCF) transcription factor mutant *msd1* had 50% less JA than WT plants and showed double the grain number per panicle. Meanwhile, application of exogenous JA can rescue the *msd1* phenotype in sorghum (Jiao et al., 2018). *Arabidopsis* mutants defective in JA biosynthesis and signaling pathway, such as *opr3*, *myc2/3/4/5*, and *coi1*, displayed a male sterility phenotype (Browse, 2009; Ishiguro et al., 2001; Qi et al., 2015; Stintzi and Browse, 2000). In our study, the exogenous JA treatment increased the expression levels of sucrose and starch synthase genes and the grain-related gene *TaGS5*, suggesting the potential effect of JA on regulation of *TaSTT3b-2B* in wheat grain weight. These investigations suggested an essential role of JA in regulating grain yield in different plant species; however, the downstream regulatory mechanisms differ in distinct taxa. These field trials were conducted in the same location for two years. In order to validate the wider applicability of the *TaSTT3b-2B* gene in wheat breeding, repeating this study while using multiple sites with different soil types and environmental conditions is needed.

Experimental procedures

Plant and fungal materials and treatments

Five wheat lines/cultivars including C112633, Shanhongmai, Yangmai158, Zhoumai18, and Wenmai 6, showing different

degrees of resistance to *R. cerealis* (Zhu *et al.*, 2015) and about 50 other cultivars with different TGWs were used in this study. The pathogenic *R. cerealis* strain, WK207, which possesses high virulence and is prevalent in northern China, was provided by Prof. Jinfeng Yu of Shandong Agricultural University, China.

All wheat plants used in this research were grown in field plots or in a greenhouse under 14-h light (22 °C)/10-h dark (12 °C) conditions (Zhu *et al.*, 2017). Wheat plants at the tillering stages were inoculated with WK207 using the toothpick inoculation method (see below). Samples were collected from leaf sheaths of wheat plants at 0, 4, 7, 14, and 21 dpi with *R. cerealis* infection and stored at –80 °C.

Sequence identification and analysis of *TaSTT3b*

Based on the sequence of TraesCS2B02G587900.1 (Ensembl Plants, <http://plants.ensembl.org/index.html>), two pairs of primers (Table S6) were designed and used for nested PCR to amplify the full-length sequences of *TaSTT3b* from cDNA and genomic DNA of CI12633 stems. The conserved motifs were predicted by an online smart software package (<http://smart.embl-heidelberg.de/>). Multiple protein sequence alignments were performed using DNAMAN software. A phylogenetic tree was constructed by using MEGA 6.0 software.

Subcellular localization of *TaSTT3b*

The coding sequence of *TaSTT3b* was amplified by the primers GFP-TaSTT3b-F/R (Table S6) and cloned into the 3' end of the GFP coding region in the p163-GFP vector to generate a GFP-TaSTT3b fusion expression vector p35S:GFP-TaSTT3b under the control of the CaMV 35S promoter. The resulting p35S:GFP-TaSTT3b construct was cotransformed into wheat protoplasts with the ER marker plasmid mCherry-HDEL (Nelson *et al.*, 2007), and transfected protoplasts were incubated at 25 °C for 20 h. Fluorescence of GFP was detected using a confocal laser scanning microscope (Zeiss LSM 700, Germany) with a fluor ×10/0.50 M27 objective lens and SP640 filter.

qRT-PCR analysis

Primers of target genes for qRT-PCR were designed by Primer Premier 5 software and are listed in Table S6. The qRT-PCR was performed using SYBR Green SuperReal PreMix (TIANGEN, China) in an ABI Prism 7500 Real-Time PCR System (Lifetech, USA). The cDNA was diluted to a 1:50 ratio with RNase-free water, and 5 µL of the diluted cDNA was used as the template. The *TaAction* gene was used as an internal control for qRT-PCR. The relative expression levels of the target genes were calculated using the comparative $2^{-\Delta\Delta CT}$ method (Livak and Schmittgen, 2001).

BSMV-induced gene silencing of *TaSTT3* in wheat CI12633

To generate the BSMV:TaSTT3a and BSMV:TaSTT3b recombinant constructs, a specific fragment (333 bp) of *TaSTT3a* and a specific fragment (192 bp) of the *TaSTT3b* gene with efficient siRNA generation were selected using Si-Fi software (Nowara *et al.*, 2010) and amplified from cDNA of CI12633. The purified PCR product digested with *Nhe* I was ligated in an antisense orientation into the RNA γ of BSMV. Clones containing the fragments in the γ -vector were confirmed by sequencing. Capped *in vitro* transcription of α -, β -, and γ -RNAs of the BSMV genome were prepared using the RiboMAX™ Large Scale RNA Production System-T7 kit (Promega, USA) and the Ribo m7G Cap Analog (Promega, USA) as described by the manufacturer's instructions. The BSMV-VIGS

experiment flowchart is shown in Figure S7a. Briefly, at the three-leaf stage, the third fully expanded leaves of CI12633 wheat plants were inoculated with *in vitro* synthesized BSMV RNAs by gently sliding pinched fingers from the leaf base to the leaf tip. BSMV:GFP served as the control. After incubation for 48 h in a humid environment (95% relative humidity), seedlings were transferred to a greenhouse under 14-h light (22 °C)/10-h dark (12 °C) conditions. After 10 dpi with BSMV, samples were collected from the fourth leaves to monitor BSMV infection based on the transcript abundance of the BSMV *cp* gene. After 20 dpi with BSMV, wheat plants were inoculated with *R. cerealis* WK207 (the inoculation method is described below). And then, seven days after *R. cerealis* inoculation, the leaf sheaths were collected and used to evaluate the transcriptional levels of target genes. The experiment was repeated three times. For one repeat, at least 15 plants were infected by BSMV:GFP, BSMV:TaSTT3a, or BSMV:TaSTT3b. The primers used in this assay are listed in Table S6.

Generation and identification of transgenic wheat

To generate the *TaSTT3b* overexpression vector, the full ORF sequence of *TaSTT3b-2B* plus a 6 × His epitope tag was amplified using the primers containing the *Bam*HI and *Sac*I restriction sites and then inserted into the monocot transformation vector pWMB122 (Wang *et al.*, 2017). In the pWMB122-TaSTT3b-2B vector (Figure S10), the TaSTT3b-2B-His fusion protein is driven by the maize ubiquitin (*Ubi*) promoter and terminated by the 3'–non-transcribed region of the *Agrobacterium tumefaciens* nopaline synthase (*Tnos*) gene. To generate *TaSTT3b* transgenic wheat plants, the pWMB122-TaSTT3b-2B vector was introduced into hexaploid wheat (cv. Zhoumai18) via *Agrobacterium*-mediated transformation. Herbicide spraying and PCR were used to select the positive transgenic plants. Herbicide spraying was performed as described by Wang *et al.* (2017). For the PCR experiment, reactions containing about 200 ng genomic DNA, 10 µL 2 × Taq MasterMix (TransGen Biotech, China), and 1 µL of each primer (10 mM) were prepared. The PCR products were resolved on a 1.5% agarose gel and visualized after ethidium bromide staining. The primers used in this assay are listed in Table S6.

Transgene copy number measurement by ddPCR

We developed a ddPCR assay using the *PINb-D1b* gene as a reference (Collier *et al.*, 2017) to estimate the copy number of the transgene. Primers and probes were designed to detect the sequence of the maize *Ubi* promoter, which was used to control *TaSTT3b-2B* expression. The *Ubi* probe was 5' FAM (6-fluorescein)-labeled and the *PINb-D1b* probe was 5' ROX (6-Carboxyl-X-Rhodamine)-labeled (Table S6). ddPCR analysis was performed using a Pilot Gene Droplet Digital PCR System (Pilot Gene Technology Company, Hangzhou, China) following the manufacturer's protocol. Briefly, the ddPCR master mix for each testing panel contained 1 × ddPCR premix, 1 µM of each primer pair (for the reference and transgene), 250 nM of each probe, and 10 µL of template DNA (~1 ng/µL), and the final volume was adjusted to 15 µL with DNase-free water. The reaction mixture was gently mixed and added into a ready-to-use disposable plastic chip to generate droplets. Chips were then amplified in a thermal cycling protocol entailed incubation at 95 °C for 5 min, followed by 40 cycles of 95 °C for 15 s and 60 °C for 1 min. After PCR amplification, chips were loaded into a chip scanner for fluorescence signal reading and further data analysis. The synthesized DNA fragment was used as a positive control, DNase-free water served as a negative control.

Western blotting assay on the transgenic wheat

Total proteins of leaf samples (0.1 g each) from the transgenic and WT wheat lines were extracted using a plant protein extraction kit (CW BIO, China). Total proteins were separated on a 12% SDS-PAGE gel and then transferred to a PVDF membrane (Millipore, USA). The TaSTT3b-2B-His protein was incubated with 2000-fold diluted anti-His antibody followed by a secondary antibody conjugated to horseradish peroxidase (HRP). After incubating overnight at 4 °C, the TaSTT3b-2B-His protein was visualized using the Pro-light HRP Chemiluminescent Kit (TIAN-GEN, China).

R. cerealis inoculation and wheat sharp eyespot evaluation

The *R. cerealis* isolate WK207 was used to inoculate wheat plants by two methods, the toothpick inoculation and wheat kernel inoculation methods. An aliquot of the fungal stock, maintained on potato dextrose agar (PDA) at 4 °C, was activated on fresh PDA plates under artificial incubation at 25 °C in the darkness (Figure S19a). For the toothpick inoculation method, according to the method of Ren *et al.* (2020) with slight modification, ordinary wooden toothpicks were cut into approximately 0.5-cm-long pieces and then autoclaved at 121 °C for 20 min. About 50 sterilized toothpick segments were evenly placed onto each PDA plate under a strict asepsis procedure. A piece of active medium with WK207 mycelia was symmetrically added to each PDA plate with toothpick segments, and then the plates were placed in an incubator at 25 °C in the darkness. After 15 days, the colonized toothpick segments were used to inoculate each stem of wheat plants (Figure S19b). The inoculated region on the stems was wrapped with wet cotton and sprayed with water twice per day during the first week and then once a day until the final disease was recorded. For the wheat kernel inoculation method, the wheat kernels were first soaked in water overnight and then transferred into Erlenmeyer flasks for autoclaving at 121 °C for 20 min. After cooling, five pieces of activated medium with WK207 mycelia were placed into each Erlenmeyer flask and mixed thoroughly before being placed in the incubator to grow at 25 °C in the darkness. The flasks were fully shaken every two days to promote uniform colonization. After 15 days, the kernels full of white mycelia were used to inoculate wheat seedlings. At the tillering growth stage, the WT and transgenic wheat plants were inoculated at the base of each stem with 8–10 colonized wheat kernels with *R. cerealis* mycelia (Figure S19c). For successful infection, the wheat field was then watered to maintain the humidity needed to facilitate infection.

As described by Zhu *et al.* (2015), based on the disease lesion widths on the base stems, ITs were categorized from 0 to 5. Disease index = $\{(0 \times X_0 + 1 \times X_1 + 2 \times X_2 + 3 \times X_3 + 4 \times X_4 + 5 \times X_5) / [(X_0 + X_1 + X_2 + X_3 + X_4 + X_5) \times 5]\} \times 100$, where X_0 – X_5 indicated plants with IT: 0–5. The representative symptom of each IT is shown in Figure S19d (Zhu *et al.*, 2015). The ITs and disease indexes of wheat plants for each line/cultivar were assessed at 14 and 28 dpi with *R. cerealis* and at harvest.

JA and DIECA treatments

Seedlings at the four-leaf stage of WT Zhoumai18 plants were sprayed with 0.1 mM MeJA plus 0.1% (v/v) Tween-20. Plants sprayed with water containing 0.1% Tween-20 were used as a control for all treatments. Leaf samples were harvested at 0, 0.5, 1, 2, 4, and 8 h post JA treatment, immediately frozen in liquid

nitrogen, and stored at –80 °C prior to total RNA extraction. C112633 plants at 20 dpi with BSMV:GFP or BSMV:TaSTT3b were sprayed with 0.1 mM MeJA plus 0.1% (v/v) Tween-20. TaSTT3b-2B transgenic and WT plants at the four-leaf stage were sprayed with 0.1 mM DIECA plus 0.1% (v/v) Tween-20. They were subsequently infected with *R. cerealis*. At 4 dpi with *R. cerealis*, leaf sheath samples were harvested and used to determine *R. cerealis* biomass.

JA measurement

For quantifying the content of JA, approximately, 0.5 g of leaf sheath tissue was harvested from seedlings of TaSTT3b-2B transgenic and WT lines at 4 dpi with *R. cerealis* infection and tested using an HPLC-MS/MS system as previously reported (Xu *et al.*, 2016). JA content of seedlings without *R. cerealis* infection was also measured as the control.

Transcriptome analysis of transgenic wheat after *R. cerealis* infection

The transcriptomes of three TaSTT3b-2B transgenic lines (OX49, OX74, and OX89) and WT Zhoumai18 were examined using RNA-seq analysis. At 4 dpi with *R. cerealis* infection, sheaths were collected from wheat seedlings and used for RNA-seq analysis. Three replicates were used. Total RNA was extracted using TRIzol (Invitrogen, California, USA) following the manufacturer's protocol. RNA integrity was evaluated using a 2100 Bioanalyzer (Agilent Technologies, California, USA). Samples with an RNA Integrity Number (RIN) ≥ 7 were selected for subsequent analysis. The RNA-seq analysis was completed by Biomarker Biotechnology (Beijing, China). The filtered clean reads were mapped to the wheat reference genome and genes (http://plants.ensembl.org/Triticum_aestivum/Info/Index). Thresholds of FDR < 0.05 and a log₂ fold change > 2 or < 0.5 were used to confirm DEGs between transgenic lines and WT Zhoumai18. Gene Ontology analysis and Kyoto Encyclopedia of Genes and Genomes pathway analyses were carried out using BMKCloud (www.biocloud.net).

Analyses of TaSTT3b-2B expression and grain weight in various wheat varieties

Seeds of various wheat varieties were planted at the experimental farm in Beijing, one variety in three repeated rows, each with a length of 1.5 m and a spacing of 25 cm. At the three-leaf stage, leaves of at least ten plants per variety were collected and mixed for qRT-PCR analysis of TaSTT3b-2B. The method of qRT-PCR refers to the "qRT-PCR analysis" section. Mature seeds were harvested and seeds from at least 20 plants for each variety were mixed for phenotypic assessment. A Seed Counter-G system (WSeen, China) was used to measure grain weight, grain width, and grain length. Three replicates were used, each with approximately 20 g seeds.

Measurements of agronomic traits

Wild type Zhoumai18 and T₃ generation plants of transgenic wheat lines (OX49, OX74, and OX89) were grown at the experimental farm at the Institute of Crop Sciences, Chinese Academy of Agricultural Sciences, Beijing, China (39°93'N, 116°40'E). The planting area of each line was 13.5 m² (Figure S20). Spike number per m², spike length, spikelet number per spike, and grain number per spike were measured as described previously by Ulukan and Kun (2007) prior to harvest. After harvest, at least 300 grains were randomly selected from each line and used to measure average grain length, grain width, and TGW

using a Seed Counter-G system (WSeen, China). The measurements of agronomic traits described above were performed with three replicates, and each contained at least 20 plants.

Acknowledgements

We appreciate Dr. Mei Niu (Institute of Crop Sciences, Chinese Academy of Agricultural Sciences) for helping us measure average grain length, grain width, and thousand-grain weight. We thank Prof. Youzhi Ma and Ms. Lina Zhang (Core Facility Platform, Institute of Crop Sciences, Chinese Academy of Agricultural Sciences) for supporting in the use of qRT-PCR and ddPCR instruments. This research was supported by grants from the National Natural Science Foundation of China (31701427, 32172004), Young Elite Scientists Sponsorship Program by CAST (2018QNRC001), and the National Key Project for Research on Transgenic Biology (2016ZX08002-001-004).

Conflict of interest

The authors declare no competing interests.

Author contributions

Z.Z. and X.Z. conceived the study, designed the experiments, and wrote the manuscript. X.Z. performed most of the experiments. X.Z. and W.R. identified the *TaSTT3b* gene. K.W. performed subcellular localization analysis of TaSTT3b-2B. W.G., M.Z., J.W., and X.W. participated in phenotyping the transgenic wheat. X.Y. provided technical assistance on wheat transformation.

References

Aebi, M. (2013) N-linked protein glycosylation in the ER. *BBA-Mol. Cell Res.* **1833**, 2430–2437.

Bari, R. and Jones, J. (2009) Role of plant hormones in plant defence responses. *Plant Mol. Biol.* **69**, 473–488.

Browse, J. (2009) The power of mutants for investigating jasmonate biosynthesis and signaling. *Phytochemistry*, **70**, 1539–1546.

Chen, C.J., Wang, J.X., Luo, Q.Q., Yuan, S.K. and Zhou, M.G. (2007) Characterization and fitness of carbendazim-resistant strains of *Fusarium graminearum* (wheat scab). *Pest Manag. Sci.* **63**, 1201–1207.

Chen, J., Li, G.H., Du, Z.Y., Quan, W., Zhang, H.Y., Che, M.Z., Wang, Z. *et al.* (2013) Mapping of QTL conferring resistance to sharp eyespot (*Rhizoctonia cerealis*) in bread wheat at the adult plant growth stage. *Theor. Appl. Genet.* **126**, 2865–2878.

Chen, L., Zhang, L., Xiang, S., Chen, Y., Zhang, H. and Yu, D. (2021) The transcription factor WRKY75 positively regulates jasmonate-mediated plant defense to necrotrophic fungal pathogens. *J. Exp. Bot.* **72**, 1473–1489.

Chen, L., Zhang, Z., Liang, H., Liu, H., Du, L., Xu, H. and Xin, Z. (2008) Overexpression of *TiERF1* enhances resistance to sharp eyespot in transgenic wheat. *J. Exp. Bot.* **59**, 4195–4204.

Chen, Y., Yan, Y., Wu, T.T., Zhang, G.L., Yin, H., Chen, W., Wang, S. *et al.* (2020) Cloning of wheat *keto-acyl thiolase 2B* reveals a role of jasmonic acid in grain weight determination. *Nat. Commun.* **11**, 6266.

Clarkson, J. D. S. and Cook, R. J. (1983) Effect of sharp eyespot (*Rhizoctonia cerealis*) on yield loss in winter wheat. *Plant Pathol.*, **32**, 421–428. <http://dx.doi.org/10.1111/j.1365-3059.1983.tb02856.x>

Collier, R., Dasgupta, K., Xing, Y.P., Hernandez, B.T., Shao, M., Rohozinski, D., Kovak, E. *et al.* (2017) Accurate measurement of transgene copy number in crop plants using droplet digital PCR. *Plant J.* **90**, 1014–1025.

Crome, M.G., Butler, R.C., Boddington, H.J. and Moorhead, A.R. (2002) Effects of sharp eyespot on yield of wheat (*Triticum aestivum*) in New Zealand. *New Zeal. J. Crop Hort.* **30**, 9–17.

Daba, S.D., Tyagi, P., Brown-Guedira, G. and Mohammadi, M. (2018) Genome-wide association studies to identify loci and candidate genes controlling kernel weight and length in a historical United States wheat population. *Front. Plant Sci.* **9**, 1045.

Fan, C., Wang, G., Wang, Y., Zhang, R., Wang, Y., Feng, S., Luo, K. *et al.* (2019) Sucrose synthase enhances hull size and grain weight by regulating cell division and starch accumulation in transgenic rice. *Int. J. Mol. Sci.* **20**, 4971.

Gao, M., Wang, X., Wang, D., Xu, F., Ding, X., Zhang, Z., Bi, D. *et al.* (2009) Regulation of cell death and innate immunity by two receptor-like kinases in Arabidopsis. *Cell Host Microbe*, **6**, 34–44.

Hammouda, A.M. (2003) First report of sharp eyespot of wheat in Egypt. *Plant Dis.* **87**, 598.

Häweker, H., Rips, S., Koiba, H., Salomon, S., Saijo, Y., Chinchilla, D., Robatzek, S. *et al.* (2010) Pattern recognition receptors require N-glycosylation to mediate plant immunity. *J. Biol. Chem.* **285**, 4629–4636.

He, K., Gou, X.P., Yuan, T., Lin, H.H., Asami, T., Yoshida, S., Russell, S.D. *et al.* (2007) BAK1 and BKK1 regulate brassinosteroid-dependent growth and brassinosteroid independent cell-death pathways. *Curr. Bio.* **17**, 1109–1115.

Hou, J., Jiang, Q., Hao, C., Wang, Y., Zhang, H. and Zhang, X. (2014) Global selection on sucrose synthase haplotypes during a century of wheat breeding. *Plant Physiol.* **164**, 1918–1929.

Ishiguro, S., Kawai-Oda, A., Ueda, J., Nishida, I. and Okada, K. (2001) The *DEFECTIVE IN ANTHER DEHISCENCE* gene encodes a novel phospholipase A1 catalyzing the initial step of jasmonic acid biosynthesis, which synchronizes pollen maturation, anther dehiscence, and flower opening in Arabidopsis. *Plant Cell*, **13**, 2191–2209.

Jeong, I.S., Lee, S., Bonkhofer, F., Tolley, J., Fukudome, A., Nagashima, Y., May, K. *et al.* (2018) Purification and characterization of *Arabidopsis thaliana* oligosaccharyltransferase complexes from the native host: a protein super-expression system for structural studies. *Plant J.* **94**, 131–145.

Jia, X., Zeng, H., Bose, S.K., Wang, W. and Yin, H. (2020) Chitosan oligosaccharide induces resistance to *Pst* DC3000 in Arabidopsis via a non-canonical N-glycosylation regulation pattern. *Carbohydr. Polym.* **250**, 116939.

Jiang, L.Y., Zhu, X., Chen, J.M., Yang, D.Y., Zhou, C.F. and Hong, Z. (2015) Two conserved oligosaccharyltransferase catalytic subunits required for N-glycosylation exist in *Spartina alterniflora*. *Bot. Stud.* **56**, 31.

Jiang, Q., Hou, J., Hao, C., Wang, L., Ge, H., Dong, Y. and Zhang, X. (2011) The wheat (*T. aestivum*) *sucrose synthase 2* gene (*TaSus2*) active in endosperm development is associated with yield traits. *Funct. Integr. Genomics*, **11**, 49–61.

Jiang, Y., Zhu, F., Cai, S., Wu, J. and Zhang, Q. (2016) Quantitative trait loci for resistance to sharp eyespot (*Rhizoctonia cerealis*) in recombinant inbred wheat lines from the cross Niavt 14 × Xuzhou 25. *Czech J. Genet. Plant*, **52**, 139–144.

Jiao, Q.S., Chen, T.S., Niu, G.T., Zhang, H.C., Zhou, C.F. and Hong, Z. (2020) N-glycosylation is involved in stomatal development by modulating the release of active abscisic acid and auxin in Arabidopsis. *J. Exp. Bot.* **71**, 5865–5879.

Jiao, Y., Lee, Y.K., Gladman, N., Chopra, R., Christensen, S.A., Regulski, M., Burrow, G. *et al.* (2018) MSD1 regulates pedicellate spikelet fertility in sorghum through the jasmonic acid pathway. *Nat. Commun.* **9**, 822.

Kemmerling, B., Schwedt, A., Rodriguez, P., Mazzotta, S., Frank, M., Qamar, S.A., Mengiste, T., Betsuyaku, S., Parker, J. E., Müssig, C., Thomma, B.P.H.J., Albrecht C., de Vries, S.C., Hirt, H., Nürnberger, T. (2007) The BRI1-Associated Kinase 1, BAK1, Has a Brassinolide-Independent Role in Plant Cell-Death Control. *Current Biology*, **17**(13), 1116–1122. <http://dx.doi.org/10.1016/j.cub.2007.05.046>

Koiba, H., Li, F., McCully, M.G., Mendoza, I., Koizumi, N., Manabe, Y., Nakagawa, Y. *et al.* (2003) The STT3a subunit isoform of the Arabidopsis oligosaccharyltransferase controls adaptive responses to salt/osmotic stress. *Plant Cell*, **15**, 2273–2284.

Lerouge, P., Cabanes-Macheteau, M., Rayon, C., Fischette-Laine, A.C., Gomord, V. and Faye, L. (1998) N-glycoprotein biosynthesis in plants: recent developments and future trends. *Plant Mol. Biol.* **38**, 31–48.

Li, Y., Fan, C., Xing, Y., Jiang, Y., Luo, L., Sun, L., Shao, D. *et al.* (2011) Natural variation in *G55* plays an important role in regulating grain size and yield in rice. *Nat. Genet.* **43**, 1266–1269.

- Li, Y.J., Yu, Y., Liu, X., Zhang, X.S. and Su, Y.H. (2021) The Arabidopsis MATERNAL EFFECT EMBRYO ARREST45 protein modulates maternal auxin biosynthesis and controls seed size by inducing AINTEGUMENTA. *Plant Cell*, **33**, 1907–1926.
- Li, Y., Zheng, L., Corke, F., Smith, C. and Bevan, M.W. (2008) Control of final seed and organ size by the DA1 gene family in *Arabidopsis thaliana*. *Genes Dev.* **22**, 1331–1336.
- Liebminger, E., Huttner, S., Vavra, U., Fischl, R., Schoberer, J., Grass, J., Blaukopf, C. et al. (2009) Class I α -mannosidases are required for N-glycan processing and root development in *Arabidopsis thaliana*. *Plant Cell*, **21**, 3850–3867.
- Liu, B., Lu, Y., Xin, Z. and Zhang, Z. (2009) Identification and antifungal assay of a wheat beta-1, 3-glucanase. *Biotechnol. Lett.* **31**, 1005–1010.
- Liu, C., Chen, L., Zhao, R., Li, R., Zhang, S., Yu, W., Sheng, J. et al. (2019) Melatonin induces disease resistance to *Botrytis cinerea* in tomato fruit by activating jasmonic acid signaling pathway. *J. Agric. Food Chem.* **67**, 6116–6124.
- Liu, C., Guo, W., Zhang, Q., Fu, B., Yang, Z., Sukumaran, S., Cai, J. et al. (2021) Genetic dissection of adult plant resistance to sharp eyespot using an updated genetic map of Niavt14 x Xuzhou25 winter wheat recombinant inbred line population. *Plant Dis.* **105**, 997–1005.
- Liu, J.X. and Howell, S.H. (2010) Endoplasmic reticulum protein quality control and its relationship to environmental stress responses in plants. *Plant Cell*, **22**, 2930–2942.
- Liu, X., Zhu, X., Wei, X., Lu, C., Shen, F., Zhang, X. and Zhang, Z. (2020) The wheat LLM-domain-containing transcription factor TaGATA1 positively modulates host immune response to *Rhizoctonia cerealis*. *J. Exp. Bot.* **71**, 344–355.
- Livak, K.J. and Schmittgen, T.D. (2001) Analysis of relative gene expression data using real-time quantitative PCR and the $2^{-\Delta\Delta CT}$ method. *Methods*, **25**, 402–408.
- Lu, H., Fermaintt, C.S., Cherepanova, N.A., Gilmore, R., Yan, N. and Lehrman, M.A. (2018) Mammalian STT3A/B oligosaccharyltransferases segregate N-glycosylation at the translocon from lipid-linked oligosaccharide hydrolysis. *Proc. Natl. Acad. Sci. USA*, **115**, 9557–9562.
- Lyons, R., Manners, J.M. and Kazan, K. (2013) Jasmonate biosynthesis and signaling in monocots: a comparative overview. *Plant Cell Rep.* **32**, 815–827.
- McGrath, K.C., Dombrecht, B., Manners, J.M., Schenk, P.M., Edgar, C.I., Maclean, D.J., Scheible, W.-R. et al. (2005) Repressor- and activator-type ethylene response factors functioning in jasmonate signaling and disease resistance identified via a genome-wide screen of *Arabidopsis transcription* factor gene expression. *Plant Physiol.* **139**, 949–959.
- Nagashima, Y., von Schaewen, A. and Koiva, H. (2018) Function of N-glycosylation in plants. *Plant Sci.* **274**, 70–79.
- Nelson, B.K., Cai, X. and Nebenfuhr, A. (2007) A multicolored set of in vivo organelle markers for co-localization studies in Arabidopsis and other plants. *Plant J.* **51**, 1126–1136.
- Nowara, D., Gay, A., Lacomme, C., Shaw, J., Ridout, C., Douchkov, D., Hensel, G. et al. (2010) HIGS: host-induced gene silencing in the obligate biotrophic fungal pathogen *Blumeria graminis*. *Plant Cell*, **22**, 3130–3141.
- de Oliveira, M.V., Xu, G., Li, B., de Souza Vespoli, L., Meng, X., Chen, X., Yu, X. et al. (2016) Specific control of Arabidopsis BAK1/SERK4-regulated cell death by protein glycosylation. *Nat. Plants*, **2**, 15218.
- Peng, X.X., Hu, Y.J., Tang, X.K., Zhou, P.L., Deng, X.B., Wang, H.H. and Guo, Z.J. (2012) Constitutive expression of rice WRKY30 gene increases the endogenous jasmonic acid accumulation, PR gene expression and resistance to fungal pathogens in rice. *Planta*, **236**, 1485–1498.
- Peng, X., Wang, H., Jang, J.C., Xiao, T., He, H., Jiang, D. and Tang, X. (2016) OsWRKY80-OsWRKY4 module as a positive regulatory circuit in rice resistance against *Rhizoctonia solani*. *Rice*, **9**, 63.
- Pieterse, C.M., Leon-Reyes, A., Van der Ent, S. and Van Wees, S.C. (2009) Networking by small-molecule hormones in plant immunity. *Nat. Chem. Biol.* **5**, 308–316.
- Qi, T., Huang, H., Song, S. and Xie, D. (2015) Regulation of jasmonate-mediated stamen development and seed production by a bHLH-MYB complex in Arabidopsis. *Plant Cell*, **27**, 1620–1633.
- Ren, Y., Yu, P.B., Wang, Y., Hou, W.X., Yang, X., Fan, J.L., Wu, X.H. et al. (2020) Development of a rapid approach for detecting sharp eyespot resistance in seedling-stage wheat and its application in Chinese wheat cultivars. *Plant Dis.* **104**, 1662–1667.
- Riemann, M., Haga, K., Shimizu, T., Okada, K., Ando, S., Mochizuki, S., Nishizawa, Y. et al. (2013) Identification of rice *Allene Oxide Cyclase* mutants and the function of jasmonate for defence against *Magnaporthe oryzae*. *Plant J.* **74**, 226–238.
- Ruiz-Canada, C., Kelleher, D.J. and Gilmore, R. (2009) Cotranslational and posttranslational N-glycosylation of polypeptides by distinct mammalian OST isoforms. *Cell*, **136**, 272–283.
- Saijo, Y., Tintor, N., Lu, X., Rauf, P., Pajerowska-Mukhtar, K., Häweker, H., Dong, X. et al. (2009) Receptor quality control in the endoplasmic reticulum for plant innate immunity. *EMBO J.* **28**, 3439–3449.
- Singh, U.B., Malviya, D., Singh, S., Kumar, M., Sahu, P.K., Singh, H.V., Kumar, S. et al. (2019) Trichoderma harzianum- and methyl jasmonate-induced resistance to *Bipolaris sorokiniana* through enhanced phenylpropanoid activities in Bread Wheat (*Triticum aestivum* L.). *Front. Microbiol.* **10**, 1697.
- Stintzi, A. and Browse, J. (2000) The Arabidopsis male-sterile mutant, *opr3*, lacks the 12-oxophytodienoic acid reductase required for jasmonate synthesis. *Proc. Natl. Acad. Sci. USA*, **97**, 10625–10630.
- Su, Z., Hao, C., Wang, L., Dong, Y. and Zhang, X. (2011) Identification and development of a functional marker of TaGW2 associated with grain weight in bread wheat (*Triticum aestivum* L.). *Theor. Appl. Genet.* **122**, 211–223.
- Sun, S., Wang, L., Mao, H., Shao, L., Li, X., Xiao, J., Ouyang, Y. et al. (2018) A G-protein pathway determines grain size in rice. *Nat. Commun.* **9**, 851.
- Taheri, P. and Tarighi, S. (2010) Riboflavin induces resistance in rice against *Rhizoctonia solani* via jasmonate-mediated priming of phenylpropanoid pathway. *J. Plant Physiol.* **167**, 201–208.
- Thomma, B.P., Eggermont, K., Penninckx, I.A., Mauch-Mani, B., Vogelsang, R., Cammue, B.P. and Broekaert, W.F. (1998) Separate jasmonate-dependent and salicylate-dependent defense-response pathways in Arabidopsis are essential for resistance to distinct microbial pathogens. *Proc. Natl. Acad. Sci. USA*, **95**, 15107–15111.
- Ulukan H., Kun E. (2007) Effect of Between and on Row Distance of First Development, Tillering, Yield and Yield Components in Wheat Cultivars (*Triticum* sp.). *Pakistan Journal of Biological Sciences*, **10**(24), 4354–4364. <http://dx.doi.org/10.3923/pjbs.2007.4354.4364>
- Wang, K., Liu, H.Y., Du, L.P. and Ye, X.G. (2017) Generation of marker-free transgenic hexaploid wheat via an *Agrobacterium*-mediated co-transformation strategy in commercial Chinese wheat varieties. *Plant Biotechnol. J.* **15**, 614–623.
- Wang, M., Zhu, X., Wang, K., Lu, C., Luo, M., Shan, T. and Zhang, Z. (2018) A wheat caffeic acid 3-O-methyltransferase TaCOMT-3D positively contributes to both resistance to sharp eyespot disease and stem mechanical strength. *Sci. Rep.* **8**, 6543.
- Wei, X., Shen, F., Hong, Y., Rong, W., Du, L., Liu, X., Xu, H. et al. (2016) The wheat calcium-dependent protein kinase TaCPK7-D positively regulates host resistance to sharp eyespot disease. *Mol. Plant Pathol.* **17**, 1252–1264.
- Wu, X.J., Cheng, K., Zhao, R.H., Zang, S.J., Bie, T.D., Jiang, Z.N., Wu, R.L. et al. (2017) Quantitative trait loci responsible for sharp eyespot resistance in common wheat C12633. *Sci. Rep.* **7**, 11799.
- Xia, T., Li, N., Dumenil, J., Li, J., Kamenski, A., Bevan, M.W., Gao, F. et al. (2013) The ubiquitin receptor DA1 interacts with the E3 ubiquitin ligase DA2 to regulate seed and organ size in Arabidopsis. *Plant Cell*, **25**, 3347–3359.
- Xie, G., Li, Z., Ran, Q., Wang, H. and Zhang, J. (2018) Over-expression of mutated *ZmDA1* or *ZmDAR1* gene improves maize kernel yield by enhancing starch synthesis. *Plant Biotechnol. J.* **16**, 234–244.
- Xu, Q., Truong, T.T., Barrero, J.M., Jacobsen, J.V., Hocart, C.H. and Gubler, F. (2016) A role for jasmonates in the release of dormancy by cold stratification in wheat. *J. Exp. Bot.* **67**, 3497–3508.
- Xu, R., Duan, P., Yu, H., Zhou, Z., Zhang, B., Wang, R., Li, J. et al. (2018) Control of grain size and weight by the OsMKK10-OsMKK4-OsMAPK6 signaling pathway in rice. *Mol. Plant*, **11**, 860–873.
- Yin, W., Xiao, Y., Niu, M., Meng, W., Li, L., Zhang, X., Liu, D. et al. (2020) ARGONAUTE2 enhances grain length and salt tolerance by activating BIG GRAIN3 to modulate cytokinin distribution in Rice. *Plant Cell*, **32**, 2292–2306.
- You, X., Zhu, S., Zhang, W., Zhang, J., Wang, C., Jing, R., Chen, W. et al. (2019) OsPEX5 regulates rice spikelet development through modulating jasmonic acid biosynthesis. *New Phytol.* **224**, 712–724.

- Zhang, Q., Sun, T. and Zhang, Y. (2015) ER quality control components UGGT and STT3a are required for activation of defense responses in *bir1-1*. *PLoS One*, **10**, e0120245.
- Zhang, Z., Yao, W., Dong, N., Liang, H., Liu, H. and Huang, R. (2007) A novel ERF transcription activator in wheat and its induction kinetics after pathogen and hormone treatments. *J. Exp. Bot.* **58**, 2993–3003.
- Zhu, X., Qi, L., Liu, X., Cai, S., Xu, H., Huang, R., Li, J. *et al.* (2014) The wheat ethylene response factor transcription factor pathogen-induced ERF1 mediates host responses to both the necrotrophic pathogen *Rhizoctonia cerealis* and freezing stresses. *Plant Physiol.* **164**, 1499–1514.
- Zhu, X., Wang, Y., Su, Z., Lv, L. and Zhang, Z. (2018) Silencing of the wheat protein phosphatase 2A catalytic subunit TaPP2Ac enhances host resistance to the necrotrophic pathogen *Rhizoctonia cerealis*. *Front. Plant. Sci.* **9**, 1437.
- Zhu, X. L., Lu, C. G., Du, L. P., Ye, X. G., Liu, X. X., Coules, A., Zhang, Z. Y. *et al.* (2017) The wheat NB-LRR gene *TaRCR1* is required for host defence response to the necrotrophic fungal pathogen *Rhizoctonia cerealis*. *Plant Biotechnology Journal*, **15**(6), 674–687. <http://dx.doi.org/10.1111/pbi.12665>
- Zhu, X., Yang, K., Wei, X., Zhang, Q., Rong, W., Du, L., Ye, X. *et al.* (2015) The wheat AGC kinase TaAGC1 is a positive contributor to host resistance to the necrotrophic pathogen *Rhizoctonia cerealis*. *J. Exp. Bot.* **66**, 6591–6603.

Supporting information

Additional supporting information may be found online in the Supporting Information section at the end of the article.

- Figure S1** Expression patterns of *TaSTT3a* from the wheat line CI12633 at 0, 4, 7, 10, 14, and 21 days post infection with *R. cerealis*.
- Figure S2** Alignment of TaSTT3b homologs of AtSTT3b and OsSTT3b.
- Figure S3** Alignment of *TaSTT3b* genomic sequences from CI12633 and Zhoumai18.
- Figure S4** Identified QTLs controlling wheat resistance to sharp eyespot.
- Figure S5** Subcellular localization of the TaSTT3b-2B protein.
- Figure S6** Schematics of genomic RNAs of the BSMV construct and the construct of the recombinant virus expressing the wheat gene TaSTT3b, BSMV: TaSTT3b.

Figure S7 BSMV-VIGS experiment flowchart and off-target prediction of *TaSTT3a* and *TaSTT3b* VIGS fragments.

Figure S8 Silencing of *TaSTT3a* by barley stripe mosaic virus-induced gene silencing in the sharp eyespot-resistant wheat line CI12633.

Figure S9 Response to *Rhizoctonia cerealis* by *TaSTT3a*-silenced and control wheat lines.

Figure S10 Diagram of *TaSTT3b-2B* overexpressing transformation vector pWMB122-TaSTT3b-2B.

Figure S11 PCR detection of *TaSTT3b-2B* in the T₀ generation of transgenic lines.

Figure S12 Droplets visualized in two dimensions for transgenic and wild type lines.

Figure S13 Volcano map of differentially expressed genes.

Figure S14 Classification of differentially expressed genes by Gene Ontology analysis.

Figure S15 GDSL-like lipase genes in differentially expressed genes.

Figure S16 Transcription analysis of eight defense-related genes in *TaSTT3b*-silenced and control wheat plants.

Figure S17 Yield-affected factors of WT and transgenic plants infected by *Rhizoctonia cerealis*.

Figure S18 Expression patterns of eight defense-related genes in wheat response to exogenous JA.

Figure S19 Schematic diagram of seedling inoculation identification for sharp eyespot.

Figure S20 Examples of field plots of wheat grown to obtain agronomic trait data.

Table S1 Identities between amino acids of TaSTT3b-2A, TaSTT3b-2B, and TaSTT3b-2D.

Table S2 Genes expressed in all samples.

Table S3 List of differentially expressed genes.

Table S4 List of defense-related genes in differentially expressed genes.

Table S5 List of genes involved in JA biosynthesis in differentially expressed genes.

Table S6 List of primers.